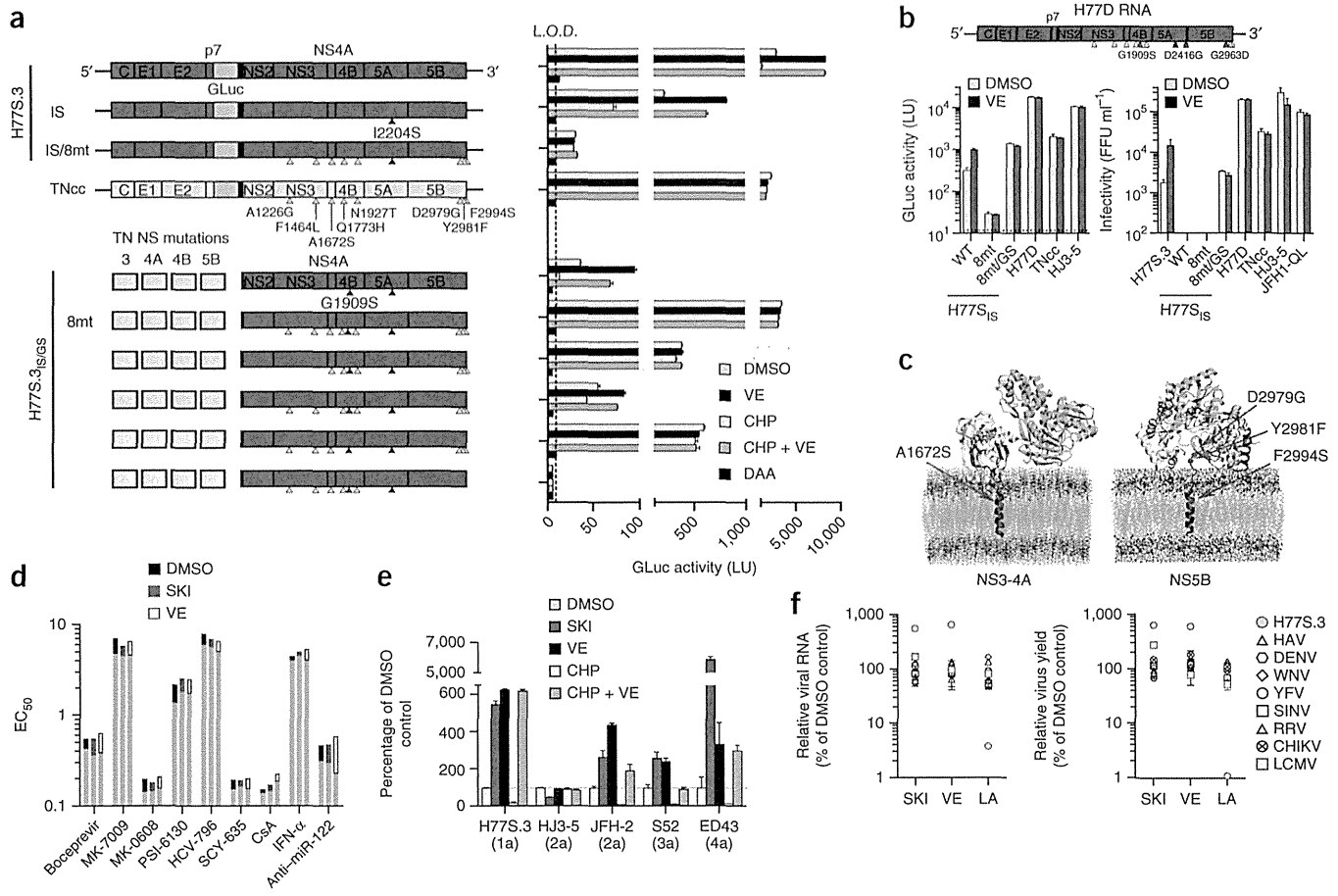


**Figure 6** Resistance to lipid peroxidation is tightly linked to robust replication in cell culture. (**a**) Top, cell culture–adaptive mutations in TNcc[34] (yellow arrowheads) that confer resistance to lipid peroxidation when introduced into H77S.3/GLuc$_{IS}$ (H77S.3/GLuc, in which the adaptive mutation S2204I has been removed (black arrowheads); details are shown in **Supplementary Fig. 10b**). GLuc produced from Huh-7.5 cells transfected with indicated RNAs and treated with DMSO, 1 μM SKI, 1 μM vitamin E, 10 μM CHP, CHP plus vitamin E or 30 μM sofosbuvir (DAA). GLuc secreted between 48–72 h is shown. Bottom, role played by TNcc mutations in NS3 (helicase) and NS4B in resistance to lipid peroxidation. Combinations of TNcc substitutions were introduced into H77S.3/GLuc$_{IS/GS}$ (NS proteins shown only) that contains the compensatory mutation G1909S (GS) in NS4B (red arrowhead, **Supplementary Fig. 11**). Data represent mean GLuc activity ± s.e.m. from two independent experiments. (**b**) Top, H77D genome containing the I2204S substitution (black arrowhead), eight TNcc-derived mutations (yellow arrowheads) and three additional compensatory mutations (red arrowheads) in the H77S.3 background. Bottom, GLuc (left) and infectious virus (right) released from Huh-7.5 cells transfected with the indicated RNAs encoding GLuc (left) or lacking GLuc (right) and treated with DMSO or 1 μM vitamin E. Data represent means ± s.d. from triplicate cultures harvested between 48–72 h in a representative experiment. WT, wild-type. (**c**) Structural models of NS4A (left) and NS5B (right) membrane interactions showing key residues that determine sensitivity to lipid peroxidation. (**d**) $EC_{50}$ of direct-acting versus indirect-acting antivirals against H77D in the presence of SKI or vitamin E (each 1 μM). Assays were carried out as in **Figure 5g**. (**e**) Huh-7.5 cells transfected with H77S.3/GLuc or HJ3-5/GLuc RNA, genome-length JFH-2 RNA or subgenomic RNAs (S52 and ED43) encoding firefly luciferase (FLuc) and treated with DMSO, 1 μM SKI or vitamin E, 10 μM CHP or CHP plus vitamin E. Data represent percentage GLuc (H77S.3 and HJ3-5), RNA copies (JFH-2) or FLuc activities (S52 and ED43) at 72 h relative to DMSO controls. Data represent mean ± s.e.m. from three independent experiments. (**f**) The impact of SKI or vitamin E (each 1 μM) or linoleic acid (50 μM) on the abundance of viral RNA (left) or yields of infectious virus (right), as determined for a panel of RNA viruses following infection of Huh-7.5 cells. Data are mean ± s.e.m. from three replicate cultures. Additional details are shown in **Supplementary Figure 12**. HAV, hepatitis A virus; DENV, dengue virus; WNV, West Nile virus; YFV, yellow fever virus; SINV, Sindbis virus; RRV, Ross River virus; CHIKV, Chikungunya virus; LCMV, lymphocytic choriomeningitis virus.

pathogenic positive-strand RNA viruses, including flaviviruses, picornaviruses and alphaviruses, is neither enhanced by SKI or vitamin E nor suppressed by linoleic acid (**Fig. 6f** and **Supplementary Fig. 12a–c**). This is also true for clone 13 lymphocytic choriomeningitis virus, an ambisense RNA virus that establishes persistent infections (**Fig. 6f** and **Supplementary Fig. 12d**). Thus, most viral RNA replicases have evolved in ways that prevent or mitigate the potentially negative effects of lipid peroxidation. HCV is a clear exception, suggesting that its sensitivity to lipid peroxidation may provide a distinct survival advantage.

## DISCUSSION

Lipid peroxides are formed on polyunsaturated fatty acid chains within membranes by reactive intermediates produced during oxidative stress. They alter membrane fluidity and permeability and potentially contribute to a variety of disease states[35]. The degradation products of these lipid peroxides include reactive aldehydes, such as acrolein, 4-hydroxy-2-nonenal and MDA, that add to this damage by forming adducts with membrane proteins, thereby modulating their biological activities[35,36]. To our knowledge, the opposing effects of SPHK1 and SPHK2 on lipid peroxidation that we observed

have not been noted previously; they remain unexplained. SPHK1 is predominantly cytosolic and translocates to the plasma membrane upon activation[37], whereas SPHK2 is more likely to be associated with intracellular membranes[28]. Sphingosine-1-phosphate produced by SPHK functions as a messenger in several signaling pathways and is a cofactor for enzymes involved in signal transduction and transcriptional regulation[38,39]. However, it has no effect on HCV replication in cell cultures and only minimally increases MDA abundance (**Supplementary Fig. 1c,d**).

During HCV infection, oxidative stress is caused by both host inflammatory responses and direct interactions of viral proteins with mitochondria[7,40]. Our results show that the wild-type H77c and N replicases are highly sensitive to both endogenous and PUFA-induced lipid peroxidation. Con1 and OR6, two other genotype 1 HCVs, are also inhibited by PUFA-induced peroxidation[8,41]. Given that we found that lipid peroxidation also inhibits multiple other HCV genotypes, we conclude that this sensitivity to peroxidation is a common feature of HCV.

In genotype 1a H77S.3 virus, we found that resistance to lipid peroxidation maps to residues within or near the transmembrane domains of NS4A and NS5B, key components of the replicase complex. Reactive aldehydes derived from degraded lipid peroxides could form adducts with residues within these transmembrane domains, impairing their capacity for essential interactions and thereby reducing replicase activity. The A1672S mutation promotes oligodimerization of the NS4A transmembrane domain, an interaction necessary for efficient replicase function[42]. Thus, A1672S might confer resistance to peroxidation by restoring NS4A dimerization impaired by adduct formation. Adduct formation could similarly affect the NS5B transmembrane domain. Although hypothetical, such effects could explain the changes we observed in the $EC_{50}$ of DAAs targeting NS3-4A and NS5B. Alternatively, proper membrane localization and assembly of nonstructural proteins within the replicase may require lipids esterified with nonoxidized fatty acid chains. Indeed, we found that monounsaturated fatty acid supplements such as oleic acid stimulate H77S.3/GLuc and N.2/GLuc replication but not that of JFH1 (**Supplementary Fig. 5h**). A third possibility is that lipid peroxidation could induce changes in membrane fluidity that alter replicase conformation[35].

We propose that HCV exploits lipid peroxidation as a means of autoregulating its replication and that lipid peroxides act as a brake, downregulating the efficiency of genome amplification when reaching a threshold abundance (**Supplementary Fig. 13**). Such a model suggests that HCV possesses a conserved peroxidation 'sensor', mapping in part to the transmembrane domains of NS4A and NS5B, that governs replication efficiency, thereby limiting tissue damage, reducing viral exposure to the immune system and facilitating viral persistence. Although hepatotoxicity associated with diets deficient in lipophilic antioxidants presents a technical barrier to testing this hypothesis in murine models of HCV[43], our results show that in primary human hepatocytes, HCV replication is regulated by lipid peroxidation. Related RNA viruses that are capable of establishing persistent infection appear to autorestrict replication via alternative mechanisms. For example, bovine viral diarrhea virus, a pestivirus that establishes lifelong persistence, downregulates replicase formation by limiting cleavage of its NS2-3 protein, thereby arresting RNA synthesis and enabling a noncytolytic phenotype[44]. Thus, reducing the efficiency of the replicase may be a common theme for RNA viruses that establish persistent infection.

Like most other positive-strand RNA viruses, the genotype 2a JFH1 virus is highly resistant to lipid peroxidation. This suggests that JFH1 may be a loss-of-function mutant that no longer senses lipid peroxides and autorestricts its replicase activity. Whether the original JFH1 patient isolate similarly lacked the ability to be regulated by lipid peroxidation is uncertain, as is the possibility that lack of peroxidation sensitivity contributed in some way to the fulminant hepatitis experienced by this patient[9]. Only one of the four amino acid substitutions conferring peroxidation resistance in H77S.3 (NS5B F2981) exists in JFH1, and the molecular basis of its peroxidation resistance remains to be determined. Nonetheless, our results provide a basis for understanding the robust capacity of the JFH1 virus to replicate in cell culture. Our findings also highlight the uniqueness of HCV regulation by lipid peroxidation among other pathogenic RNA viruses and its potential importance to the pathogenesis of chronic hepatitis C.

## METHODS

Methods and any associated references are available in the online version of the paper.

*Note: Any Supplementary Information and Source Data files are available in the online version of the paper.*


### ACKNOWLEDGMENTS

We thank L.F. Ping and W. Lovell for expert technical assistance, R. Purcell (US National Institute of Allergy and Infectious Diseases) and J. Bukh (Copenhagen University Hospital, Denmark) for pCV-H77C and pTNcc plasmids, C.M. Rice and M. Saeed (The Rockefeller University) for Huh-7.5 cells and S52/SG-Feo and ED43/SG-Feo plasmids, T. Wakita (National Institute of Infectious Diseases, Japan) for pJFH1 and pJFH-2 plasmids, M.J. Otto (Pharmasset) for PSI-6130, A. Sluder (SCYNEXIS) for SCY-635, R. De Francesco (Istituto Nazionale di Genetica Molecolare, Italy) for compound 23, A.Y. Howe (Merck Research Laboratory) for boceprevir, HCV-796, MK-0608 and MK-7009 and Z. Feng (University of North Carolina) for hepatitis A virus stocks. We also thank S.A. Weinman for critical reading of the manuscript and D.L. Tyrrell, M. Joyce, R.A. Coleman and T. Masaki for helpful discussions. This work was supported by US National Institutes of Health grants RO1-AI095690, RO1-CA164029 and U19-AI109965 (S.M.L.), R21-CA182322 (L.R.), R01-AI075090 (M.Y.), RO1-AI073335 (C.C.K.), RO1-DE018304 (D.P.D.), F32-AI094941 (D.G.W.) and U54-GM069338 (S.B.), a National Cancer Institute Center Core Support Grant to the Lineberger Comprehensive Cancer Center (P30-CA016086) and the University of North Carolina Cancer Research Fund. C.W. was supported by the Deutsche Forschungsgemeinschaft (WE 4388/3-1 and WE 4388/6-1). I.A. was supported by the CIPSM Cluster of Excellence.


### AUTHOR CONTRIBUTIONS

D.Y. and S.M.L. conceived the study and wrote the paper; D.Y., D.R.M., E.W., V.J.M., Y.W., P.E.C., C.E.M., D.G.W. and I.M. conducted experiments; C.W. and I.A. modeled membrane interactions of proteins; S.B. and A.H.M. Jr. carried out mass spectrometry analysis of sphingolipids; J.K.W., M.T.H., D.P.D. and C.C.K. provided reagents and supervised experiments involving viruses other than HCV; M.Y., S.K., T.S., T.O., S.M.P. and L.M.R. provided research materials; and all authors discussed the results and commented on the manuscript.

### COMPETING FINANCIAL INTERESTS

The authors declare competing financial interests: details are available in the online version of the paper.


Reprints and permissions information is available online at http://www.nature.com/reprints/index.html.



1. Kalyanaraman, B. Teaching the basics of redox biology to medical and graduate students: oxidants, antioxidants and disease mechanisms. *Redox. Biol.* **1**, 244–257 (2013).
2. Nathan, C. & Cunningham-Bussel, A. Beyond oxidative stress: an immunologist's guide to reactive oxygen species. *Nat. Rev. Immunol.* **13**, 349–361 (2013).
3. Dennery, P.A. Effects of oxidative stress on embryonic development. *Birth Defects Res. C Embryo Today* **81**, 155–162 (2007).
4. Valyi-Nagy, T. & Dermody, T.S. Role of oxidative damage in the pathogenesis of viral infections of the nervous system. *Histol. Histopathol.* **20**, 957–967 (2005).
5. Thomas, D.L. Global control of hepatitis C: where challenge meets opportunity. *Nat. Med.* **19**, 850–858 (2013).
6. Choi, J. Oxidative stress, endogenous antioxidants, alcohol, and hepatitis C: pathogenic interactions and therapeutic considerations. *Free Radic. Biol. Med.* **52**, 1135–1150 (2012).

7. Okuda, M. *et al.* Mitochondrial injury, oxidative stress, and antioxidant gene expression are induced by hepatitis C virus core protein. *Gastroenterology* **122**, 366–375 (2002).
8. Huang, H., Chen, Y. & Ye, J. Inhibition of hepatitis C virus replication by peroxidation of arachidonate and restoration by vitamin E. *Proc. Natl. Acad. Sci. USA* **104**, 18666–18670 (2007).
9. Wakita, T. *et al.* Production of infectious hepatitis C virus in tissue culture from a cloned viral genome. *Nat. Med.* **11**, 791–796 (2005).
10. Lindenbach, B.D. *et al.* Complete replication of hepatitis C virus in cell culture. *Science* **309**, 623–626 (2005).
11. Zhong, J. *et al.* Robust hepatitis C virus infection *in vitro*. *Proc. Natl. Acad. Sci. USA* **102**, 9294–9299 (2005).
12. Yi, M., Villanueva, R.A., Thomas, D.L., Wakita, T. & Lemon, S.M. Production of infectious genotype 1a hepatitis C virus (Hutchinson strain) in cultured human hepatoma cells. *Proc. Natl. Acad. Sci. USA* **103**, 2310–2315 (2006).
13. Pietschmann, T. *et al.* Production of infectious genotype 1b virus particles in cell culture and impairment by replication enhancing mutations. *PLoS Pathog.* **5**, e1000475 (2009).
14. Paul, D., Hoppe, S., Saher, G., Krijnse-Locker, J. & Bartenschlager, R. Morphological and biochemical characterization of the membranous hepatitis C virus replication compartment. *J. Virol.* **87**, 10612–10627 (2013).
15. Gosert, R. *et al.* Identification of the hepatitis C virus RNA replication complex in Huh-7 cells harboring subgenomic replicons. *J. Virol.* **77**, 5487–5492 (2003).
16. Shi, S.T., Lee, K.J., Aizaki, H., Hwang, S.B. & Lai, M.M. Hepatitis C virus RNA replication occurs on a detergent-resistant membrane that cofractionates with caveolin-2. *J. Virol.* **77**, 4160–4168 (2003).
17. Hsu, N.Y. *et al.* Viral reorganization of the secretory pathway generates distinct organelles for RNA replication. *Cell* **141**, 799–811 (2010).
18. Reiss, S. *et al.* Recruitment and activation of a lipid kinase by hepatitis C virus NS5A is essential for integrity of the membranous replication compartment. *Cell Host Microbe* **9**, 32–45 (2011).
19. Saxena, V., Lai, C.K., Chao, T.C., Jeng, K.S. & Lai, M.M. Annexin A2 is involved in the formation of hepatitis C virus replication complex on the lipid raft. *J. Virol.* **86**, 4139–4150 (2012).
20. Romero-Brey, I. *et al.* Three-dimensional architecture and biogenesis of membrane structures associated with hepatitis C virus replication. *PLoS Pathog.* **8**, e1003056 (2012).
21. Miyanari, Y. *et al.* The lipid droplet is an important organelle for hepatitis C virus production. *Nat. Cell Biol.* **9**, 1089–1097 (2007).
22. Aizaki, H. *et al.* Critical role of virion-associated cholesterol and sphingolipid in hepatitis C virus infection. *J. Virol.* **82**, 5715–5724 (2008).
23. Sakamoto, H. *et al.* Host sphingolipid biosynthesis as a target for hepatitis C virus therapy. *Nat. Chem. Biol.* **1**, 333–337 (2005).
24. Umehara, T. *et al.* Serine palmitoyltransferase inhibitor suppresses HCV replication in a mouse model. *Biochem. Biophys. Res. Commun.* **346**, 67–73 (2006).
25. Hirata, Y. *et al.* Self-enhancement of hepatitis C virus replication by promotion of specific sphingolipid biosynthesis. *PLoS Pathog.* **8**, e1002860 (2012).
26. Weng, L. *et al.* Sphingomyelin activates hepatitis C virus RNA polymerase in a genotype-specific manner. *J. Virol.* **84**, 11761–11770 (2010).
27. Shimakami, T. *et al.* Protease inhibitor-resistant hepatitis C virus mutants with reduced fitness from impaired production of infectious virus. *Gastroenterology* **140**, 667–675 (2011).
28. Liu, H. *et al.* Molecular cloning and functional characterization of a novel mammalian sphingosine kinase type 2 isoform. *J. Biol. Chem.* **275**, 19513–19520 (2000).
29. Kapadia, S.B. & Chisari, F.V. Hepatitis C virus RNA replication is regulated by host geranylgeranylation and fatty acids. *Proc. Natl. Acad. Sci. USA* **102**, 2561–2566 (2005).
30. Lindenbach, B.D. *et al.* Cell culture-grown hepatitis C virus is infectious *in vivo* and can be recultured *in vitro*. *Proc. Natl. Acad. Sci. USA* **103**, 3805–3809 (2006).
31. Yanagi, M., Purcell, R.H., Emerson, S.U. & Bukh, J. Transcripts from a single full-length cDNA clone of hepatitis C virus are infectious when directly transfected into liver of a chimpanzee. *Proc. Natl. Acad. Sci. USA* **94**, 8738–8743 (1997).
32. Beard, M.R. *et al.* An infectious molecular clone of a Japanese genotype 1b hepatitis C virus. *Hepatology* **30**, 316–324 (1999).
33. Andrus, L. *et al.* Expression of paramyxovirus V proteins promotes replication and spread of hepatitis C virus in cultures of primary human fetal liver cells. *Hepatology* **54**, 1901–1912 (2011).
34. Li, Y.P. *et al.* Highly efficient full-length hepatitis C virus genotype 1 (strain TN) infectious culture system. *Proc. Natl. Acad. Sci. USA* **109**, 19757–19762 (2012).
35. Bochkov, V.N. *et al.* Generation and biological activities of oxidized phospholipids. *Antioxid. Redox Signal.* **12**, 1009–1059 (2010).
36. Pizzimenti, S. *et al.* Interaction of aldehydes derived from lipid peroxidation and membrane proteins. *Front. Physiol.* **4**, 242 (2013).
37. Pitson, S.M. *et al.* Activation of sphingosine kinase 1 by ERK1/2-mediated phosphorylation. *EMBO J.* **22**, 5491–5500 (2003).
38. Alvarez, S.E. *et al.* Sphingosine-1-phosphate is a missing cofactor for the E3 ubiquitin ligase TRAF2. *Nature* **465**, 1084–1088 (2010).
39. Hait, N.C. *et al.* Regulation of histone acetylation in the nucleus by sphingosine-1-phosphate. *Science* **325**, 1254–1257 (2009).
40. Jain, S.K. *et al.* Oxidative stress in chronic hepatitis C: not just a feature of late stage disease. *J. Hepatol.* **36**, 805–811 (2002).
41. Yano, M. *et al.* Comprehensive analysis of the effects of ordinary nutrients on hepatitis C virus RNA replication in cell culture. *Antimicrob. Agents Chemother.* **51**, 2016–2027 (2007).
42. Kohlway, A. *et al.* Hepatitis C virus RNA replication and virus particle assembly require specific dimerization of the NS4A protein transmembrane domain. *J. Virol.* **88**, 628–642 (2014).
43. Ibrahim, W. *et al.* Oxidative stress and antioxidant status in mouse liver: effects of dietary lipid, vitamin E and iron. *J. Nutr.* **127**, 1401–1406 (1997).
44. Lackner, T., Muller, A., Konig, M., Thiel, H.J. & Tautz, N. Persistence of bovine viral diarrhea virus is determined by a cellular cofactor of a viral autoprotease. *J. Virol.* **79**, 9746–9755 (2005).

## ONLINE METHODS

**Cells and reagents.** Huh-7.5 cells were grown in Dulbecco's modified Eagle's medium (DMEM), High Glucose supplemented with 10% fetal bovine serum (FBS), 1× penicillin-streptomycin, 1× GlutaMAX and 1× MEM Non-Essential Amino Acids Solution (Gibco). BD-BioCoat collagen-I coated plates were purchased from BD Biosciences. SKI (2-(*p*-hydroxyanilino)-4-(*p*-chlorophenyl) thiazole) was obtained from Merck Millipore. Myriocin, fumonisin B1, *N*-[2-hydroxy-1-(4-morpholinylmethyl)-2-phenylethyl]-decanamide (PDMP), D-erythro-2-tetradecanoylamino-1-phenyl-1-propanol (D-MAPP), dihydrosphingosine, C-2 and C-8 ceramides, sphingosine, sphingosine 1-phosphate, lovastatin, ebselen, arachidonic acid, docosahexaenoic acid and linoleic acid were from Cayman Chemical. Vitamin E (α-, *rac*-β- and γ-tocopherols), 4-deoxypyridoxine hydrochloride (DOP), coenzyme Q10, butylated hydroxytoluene, *N*-acetyl-L-cysteine, diphenyleneiodonium chloride, oleic acid and cyclosporine A were from Sigma-Aldrich. nSMase spiroepoxide and cumene hydroperoxide were from Santa Cruz Biotechnology; D609 was from Enzo Life Sciences; and sofosbuvir (PSI-7977) was from Chemscene. Locked nucleic acid anti-miR-122 was synthesized by Exiqon. A selective PI4KIIIα inhibitor, compound 23 (ref. 45), was provided by R. De Francesco. Relative cell numbers were assessed using the WST-1 reagent (Millipore) or determination of protein content. Protein concentrations in samples were determined using the Protein Assay kit (Bio-Rad) with bovine serum albumin as a standard.

**Fetal liver cells.** Tissue samples were supplied by the accredited nonprofit corporation Advanced Biosciences Resources, Inc. (ABR) and obtained from fetuses between 15–20 weeks gestation during elective terminations of pregnancy. Tissues were collected with written informed consent from all donors and in accordance with the US Food and Drug Administration CFR Part 1271 Good Tissue Practices regulations. Tissue was processed as described elsewhere[46–48], and isolated hepatoblasts were seeded at density of $5.2 \times 10^5$ cm$^{-2}$ on 12- or 24-well plates and in regular Kubota's Medium[49] supplemented with 5% FBS. Following an overnight incubation, the medium was changed to a variation of Kubota's Medium (HFH medium) comprised of DMEM supplemented with 25 mM HEPES, 1 nM selenium, 0.1% BSA, 4.5 mM niacinamide, 0.1 nM zinc sulfate heptahydrate, 10 nM hydrocortisone, 5 μg ml$^{-1}$ transferrin/Fe, 5 μg ml$^{-1}$ insulin, 2 mM L-glutamine, antibiotics and 2% FBS. The use of commercially procured fetal liver cells was reviewed by the University of North Carolina at Chapel Hill Office of Human Research Ethics and was determined not to require approval by the University of North Carolina at Chapel Hill Institutional Review Board.

**Plasmids.** pHJ3-5 (ref. 50), pHJ3-5/GLuc2A (referred to here as pHJ3-5/GLuc), pHJ3-5/GND, pH77c (ref. 51), pH77S.3, pH77S.3/GLuc2A (referred to here as pH77S.3/GLuc) and pH77S/GLuc2A-AAG (refs. 12,27,52) have been described. pHCV-N.2 is a modified version of HCV3-9b (ref. 32) that contains cell culture–adaptive mutations in NS3 and NS5A (A1099T, E1203G and S2204I in the polyprotein). Mutations in the sphingomyelin binding domain, 5′ UTR, 3′ UTR and nonstructural protein regions were generated by site-directed mutagenesis. The *Gaussia princeps* luciferase (GLuc)-coding sequence followed by the foot-and-mouth disease virus 2A protease–coding sequence was inserted between p7 and NS2 in pH77c, pHCV-N.2, pJFH1 (wild-type) and pJFH1-QL (containing the cell culture–adaptive mutation Q221L in the NS3 helicase) using a strategy applied previously to pH77S (ref. 27). JFH1-QL was used for experiments unless otherwise indicated. Other cell culture–adapted genotype 1a (TNcc), 2a (JFH-2/AS/mtT3), 3a (S52/SG-Feo(SH)) and 4a (ED43/SG-Feo(K)) HCV strains and RNA replicons have been described[34,53,54].

**Luciferase assays.** For the *Gaussia* luciferase (GLuc) assay, cells transfected with HCV RNA encoding GLuc were treated with drugs at 6 h after transfection, and the culture medium was harvested, refed with fresh medium containing drugs and assayed for GLuc at 24-h intervals. Secreted GLuc activity was measured as described[52]. For the firefly luciferase (FLuc) assay, cell monolayers were washed with PBS and lysed in Passive Lysis Buffer (Promega), and the lysates were analyzed with the Luciferase Assay System (Promega) according to the manufacturer's instructions. For each individual experiment, we used duplicate or triplicate cell cultures. Results shown represent the mean ± s.e.m. from multiple independent experiments.

**RNA transcription.** RNA transcripts were synthesized *in vitro* as described previously[27].

**Hepatitis C virus RNA transfection.** At 24 h before transfection, $7.5 \times 10^4$ Huh-7.5 cells were seeded onto a 24-well plate. One day later, medium was replaced with fresh medium, and the cells were transfected with 0.25 μg (per well) HCV RNA–encoding GLuc using the TransIT mRNA transfection kit (Mirus) according to the manufacturer's protocol. After 6 h incubation at 37 °C, supernatant fluids were removed for GLuc assay and replaced with fresh medium-containing compound. Alternatively, 10 μg of HCV RNA was mixed with $5 \times 10^6$ Huh-7.5 cells and electroporated into cells using a Gene Pulser Xcell Total System (Bio-Rad) as described previously[52]. Transfection of wild-type HCV RNA was performed by electroporating 5 μg HCV RNA in $2.5 \times 10^6$ Huh-7.5 cells and seeded into collagen-coated plates (BD Biosciences). Cells were grown in DMEM supplemented with 25 mM HEPES, 7 ng ml$^{-1}$ glucagon, 100 nM hydrocortisone, 5 μg ml$^{-1}$ insulin, 2 mM GlutaMAX, antibiotics and 2% FBS. Culture supernatants were replaced with the medium supplemented with drugs at 6 h and every 48 h thereafter and assayed for GLuc activity.

**Hepatitis C virus production.** For virus production, subconfluent Huh-7.5 cells in a 100-mm diameter dish were transfected with 5 μg HCV RNA using the TransIT mRNA transfection kit as above and split at 1:2 ratio at 6 h after transfection. Cells were then fed with medium supplemented with 50 mM HEPES (Cellgro) and the supernatants harvested and replaced with fresh medium every 24 h. Cells were passaged at a 1:2 ratio again 3 d after transfection. Medium containing HCV was supplemented with an additional 50 mM HEPES and stored at 4 °C until assayed for infectivity. *Gaussia* luciferase H77S.3/GLuc reporter virus was produced by electroporating 5 μg H77S.3/GLuc RNA into $2.5 \times 10^6$ Huh-7.5 cells. Cells were fed with medium containing 25 mM HEPES and 10 μM vitamin E at 3 h and grown for 3 d until subconfluent. Cells were then split 1:3 into medium containing 25 mM HEPES. Supernatant fluids, harvested on the following day, were stored at 4 °C until use. HJ3-5/GLuc virus was produced in medium lacking vitamin E and stored in −80 °C until use. Infectious titers were determined by $TCID_{50}$ using GLuc activity produced at 72 h after inoculation.

**Hepatitis C virus infectivity assays.** Huh-7.5 cells were seeded at $5 \times 10^4$ cells per well into 48-well plates 24 h before inoculation with 100 μl of culture medium. Cells were fed with medium containing 1 μM vitamin E 24 h later to facilitate visualization of core protein expression, fixed with methanol-acetone (1:1) at −20 °C for 10 min 72 h after inoculation (48 h for JFH1-QL and HJ3-5) and stained for intracellular core antigen with a mouse monoclonal antibody C7–50 (Thermo Scientific, 1:300 dilution). Clusters of infected cells identified by staining for core antigen were considered to constitute a single infectious focus, and the data were expressed as focus-forming units (FFU) ml$^{-1}$.

**Hepatitis C virus infection in fetal hepatoblasts.** Cells were inoculated with HCV encoding GLuc (MOI = 0.001) for 6 h. After washing five times with HFH medium, cells were incubated for an additional 18 h to determine baseline GLuc secretion. Culture supernatant fluids were replaced at 24 h intervals with HFH medium containing drugs and assayed for GLuc.

**Flow cytometry.** Huh-7.5 cells electroporated with H77S.3 or HJ3-5 RNA were treated with 1 μM SKI or DMSO beginning at 24 h and analyzed for NS5A expression by flow cytometry at 96 h. Virus spread assays were adapted from a previously described method[55]. Briefly, Huh-7.5 cells were electroporated with H77S.3, HJ3-5 or HJ3-5/GND RNAs and cultured for 24 h. The electroporated (producer) cells were then cocultured at a 1:4 ratio with naive Huh-7.5 (recipient) cells prelabeled with 5 μM carboxyfluorescein diacetate succinimidyl ester (CellTrace CFSE Cell Proliferation Kit, Invitrogen) in the presence of different compounds (see figure legends) for 48 h. Cells were stained for NS5A protein and analyzed by flow cytometry as described previously[56].

**Equilibrium ultracentrifugation.** Filtered supernatant fluids collected from transfected cell cultures were concentrated 50-fold using Centricon Plus-70 Centrifugal Filter Units (100-kDa exclusion) (Millipore) and then layered on top of a preformed continuous 10–40% iodixanol (OptiPrep, Sigma-Aldrich)


doi:10.1038/nm.3610

gradient in Hank's balanced salt solution (HBSS, Invitrogen). Gradients were centrifuged in a SureSpin 630 Swinging Bucket Rotor (Thermo Scientific) at 30,000 r.p.m. for 24 h at 4 °C, and fractions were collected from the top of the tube. The density of each fraction was calculated from the refractive index measured with a refractometer (ATAGO). RNA was isolated from each fraction using QIAamp Viral RNA kit (Qiagen) and the viral amount quantified by qRT-PCR as described below. Infectious virus titers in each fraction were determined as described above.

**qRT-PCR.** One-step qRT-PCR analysis of HCV RNA in Huh-7.5 cells was carried out as described[52]. HCV RNA in primary human fetal hepatoblast cultures was detected by means of a two-step qRT-PCR procedure using SuperScript III First-Strand Synthesis SuperMix for qRT-PCR (Invitrogen), followed by TaqMan qPCR analysis with primer pairs and a probe targeting a conserved 221-base sequence within the 5′ UTR of the genome and iQ Supermix (Bio-Rad)[52].

**RNA interference.** Validated siRNA targeting human *SPHK1* (SI02660455)[57] was purchased from Qiagen. siRNA targeting human *SPHK2* (5′-CGUCAC GGUUAAAGAGAAA-3′)[39] and control siRNA (#2) were from Dharmacon. siRNA (20 nM) was transfected into cells using siLentfect Lipid Reagent (Bio-Rad) according to the manufacturer's protocol.

**Immunoblots.** Immunoblotting was carried out using standard methods with the following antibodies: mouse monoclonal antibodies to β-actin (AC-74, Sigma, 1:10,000), HCV NS3 (ab65407, Abcam, 1:500) and rabbit polyclonal antibodies to SPHK1 (A302-177A, Bethyl Laboratories, 1:2,000) or SPHK2 (ab37977, Abcam, 1:500). Protein bands were visualized and quantified with an Odyssey Infrared Imaging System (Li-Cor Biosciences).

**Sphingosine kinase assay.** Sphingosine kinase activity was determined as described previously[28]. Recombinant human SPHK1 and SPHK2 proteins were obtained from BPS Bioscience. SPHK1 activity was determined in the presence of 0.25% Triton X-100, which inhibits SPHK2 (ref. 28). The labeled S1P was separated by TLC on Silica Gel G-60 (Whatman) with 1-butanol/ethanol/acetic acid/water (80:20:10:20, v/v) and visualized and quantified by phosphorimager (Bio-Rad).

**Quantification of cholesterol and triglyceride levels.** Cells were scraped and lysed in PBS containing 1% Triton X-100 and complete protease inhibitor cocktail (Roche). Cell lysates were clarified by centrifugation at 15,000 r.p.m. at 4 °C for 10 min. Cholesterol contents were determined using the Amplex Red Cholesterol Assay Kit (Invitrogen) according to the manufacturer's protocol. Triglyceride levels in cells grown on 96-well plates were determined using Triglyceride Assay Kit (Zen-Bio) as per manufacturer's instruction. The values were normalized to the total protein content.

**Lipid peroxidation assays.** Malondialdehyde (MDA), a product of lipid peroxidation, was quantified by the thiobarbituric acid reactive substances (TBARS) Assay Kit (Cayman Chemical). Cells transfected with HCV RNAs were grown in the presence of different drugs and analyzed for intracellular malondialdehyde (MDA) abundance at 48–72 h as indicated in legends. Cells scraped into PBS containing complete protease inhibitor cocktail (Roche) were homogenized by sonication on ice using Sonic Dismembrator (FB-120, Fisher Scientific). The amount of MDA in 100 µl of cell homogenates was analyzed by a fluorescent method as described by the manufacturer. Lipid peroxidation levels were expressed as the amount of MDA normalized to the amount of total protein. Alternatively, the lipid peroxidation product, 8-isoprostane, was quantified using the 8-Isoprostane EIA kit (Cayman Chemical) according to the manufacturer's recommended procedures.

**Innate immune response reporter assays.** IFN-β–, IRF-3– and NF-κB–dependent promoter activities were assayed using firefly luciferase reporters pIFN-β-Luc, p4xIRF3-Luc or pPRDII-Luc as described previously[58]. Cells were cotransfected with the reporter plasmid pRL-CMV, and the firefly luciferase results were normalized to *Renilla* luciferase activity in order to control for potential differences in transfection efficiency. The luminescence was measured on a Synergy 2 (Bio-Tek) Multi-Mode Microplate Reader.

**Mass spectrometry of sphingolipids and metabolites.** Cells were washed extensively with PBS and scraped into tubes. An aliquot of cells was taken for protein and total lipid phosphate measurements. After addition of a sphingolipid internal standard cocktail (Avanti Polar Lipids), the lipids were extracted, and individual sphingolipid species were quantified by liquid chromatography, electrospray ionization-tandem mass spectrometry as described previously[59,60].

**Electron microscopy.** Huh-7.5 cells ($5 \times 10^6$ cells) electroporated with 5 µg HCV RNA were seeded into a 6-well plate, and medium containing compounds was added 24 h later. At 48 h after transfection, cells were fixed with 3% glutaraldehyde in 0.15 M sodium phosphate buffer, pH 7.4, for 1 h at room temperature and stored at 4 °C until processed. Following three rinses with 0.15 M sodium phosphate buffer, pH 7.4, monolayers were postfixed with 1% osmium tetroxide for 1 h, washed in deionized water and stained *en bloc* with 2% aqueous uranyl acetate for 20 min. The cells were dehydrated using increasing concentrations of ethanol (30%, 50%, 75%, 100%, 100%, 10 min each) and embedded in Polybed 812 epoxy resin (Polysciences, Inc.). Cell layers were sectioned *en face* to the substrate at 70 nm using a diamond knife and a Leica Ultracut UCT microtome (Leica Microsystems). Ultrathin sections were mounted on 200 mesh copper grids and stained with 4% aqueous uranyl acetate and Reynolds' lead citrate[61]. The grids were observed at 80 kV using a LEO EM910 transmission electron microscope (Carl Zeiss SMT, LLC). Digital images were taken using a Gatan Orius SC 1000 CCD Camera with DigitalMicrograph 3.11.0 software (Gatan, Inc.).

**Peroxidation resistance of hepatitis A virus, flavivirus, alphavirus and lymphocytic choriomeningitis virus replicases.** Virus stocks were provided as follows: HAV by Z. Feng and S.M.L.; YFV and WNV by D.P.D.; DENV by D.G.W.; SINV, RRV and CHIKV by M.T.H.; and LCMV by J.K.W. The abundance of HAV, RRV, SINV and LCMV RNA was determined using iScript One-Step RT-PCR kit with SYBR green (Bio-Rad) and primer pairs as follows: HAV forward 5′-GGTAGGCTACGGGTGAAAC-3′ and reverse 5′-AACAACTCACCAATATCCGC-3′, RRV forward 5′-AGAGT GCGGAAGACCCAGAG-3′ and reverse 5′-CCGTGATCTTACCGGACA CA-3′, SINV forward 5′-GAGGTAGTAGCACAGCAGG-3′, and reverse 5′-CG GAAAACATTCTACGAGC-3′ and LCMV forward 5′-CATTCACCTGGACTTT GTCAGACTC-3′ and reverse 5′-GCAACTGCTGTGTTCCCGAAAC-3′. WNV and YFV RNA levels were quantified using a previously described method[62] with primers as follows: WNV forward 5′-TCAGCGATCTCTCCACCAAAG-3′ and reverse 5′-GGGTCAGCACGTTTGTCATTG-3′ and YFV forward 5′-CT GTCCCAATCTCAGTCC-3′ and reverse 5′-AATGCTCCCTTTCCCAAA TA-3′. DENV RNA was quantified on a 7900 HT Real-Time PCR System (ABI) using primers and probe as described[63].

The infrared fluorescent immunofocus assay for infectious hepatitis A virus (HAV) was done using FRhK-4 cells as previously described[64]. Titration of infectious alphaviruses was performed in duplicate by visualization of plaques on Vero cells seeded in 12-well plates. Plates were incubated with inoculum at 37 °C with 5% $CO_2$ for 1 h with periodic agitation. Inocula were then removed and plates overlaid with 1.25% carboxymethylcellulose in MEM supplemented with 3% FBS, 1× penicillin-streptomycin, 2 mM L-glutamine and HEPES. All of these reagents were identical to those used for parallel studies of HCV. At 48 h after infection, plates were fixed with 4% paraformaldehyde and visualized with a 0.25% crystal violet solution. Infectious titers of WNV and YFV were determined by plaque assay on confluent BHK cell monolayers in 6-well plates. Cells were incubated with virus inocula for 2 h at 37 °C, washed before addition of a 1% methylcellulose medium overlay and further incubated for 3 d. Plaques were visualized with Giemsa staining. DENV titers were determined by plaque assay on Vero 76 cell monolayers in 96-well plates. Cells were incubated with virus inocula for 2 h at 37 °C, washed before addition of a 0.8% methylcellulose medium overlay and further incubated for 3 d. Following fixation with ice-cold acetone methanol solution (50:50 v/v), cells were immunostained using the DENV E–specific monoclonal antibody 4G2 (UNC Antibody Core Facility, 1:500) followed by HRP-conjugated anti-mouse IgG secondary antibody (KPL, 464-1806, 1:1,000). Infectious foci were visualized using Vector VIP reagent (Vector Labs). LCMV titers were determined by plaque assay on confluent Vero cell monolayers in 6-well plates[65]. Cells were incubated with virus inocula for 80 min at 37 °C before addition of a 1:1 mixture of 1% agarose and EMEM medium containing 10% FCS, 2 mM L-glutamine, 2% penicillin and

2% streptomycin. Cells were further incubated for 5 d at 37 °C. Plaques were visualized with crystal violet.

**Modeling of hepatitis C virus nonstructural protein-membrane interactions.** Membrane topologies of HCV nonstructural proteins were modeled as suggested by Bartenschlager *et al.*[66] using the Protein Data Bank (PDB) structure 4A92 for the NS3-4A protease-helicase (**Fig. 6c**) and PDB 1GX6 for the NS5B RNA-dependent RNA polymerase (**Fig. 6c**). Secondary structure predictions were generated on the Jpred3 server (http://www.compbio.dundee.ac.uk/www-jpred/). Visual Molecular Dynamics (VMD) with the plugin "Membrane" was applied for visualization of protein-membrane interactions[67].

**Statistical analyses.** Unless noted otherwise, all between-group comparisons were carried out by two-way ANOVA using Prism 6.0 software (GraphPad Software, Inc.). For determination of $EC_{50}$ concentrations of DAAs, data were fit to a four-parameter dose-response curve with variable slope using Prism 5.0c for Mac OS X software (GraphPad Software, Inc.). Results are reported as the estimated $EC_{50} \pm 95\%$ confidence interval (**Fig. 5g**).


45. Leivers, A.L. *et al.* Discovery of selective small molecule type iii phosphatidylinositol 4-kinase α (PI4KIIIα) inhibitors as anti hepatitis C (HCV) agents. *J. Med. Chem.* **57**, 2091–2106 (2014).
46. Oikawa, T. *et al.* Sal-like protein 4 (SALL4), a stem cell biomarker in liver cancers. *Hepatology* **57**, 1469–1483 (2013).
47. Schmelzer, E. *et al.* Human hepatic stem cells from fetal and postnatal donors. *J. Exp. Med.* **204**, 1973–1987 (2007).
48. Wang, Y. *et al.* Paracrine signals from mesenchymal cell populations govern the expansion and differentiation of human hepatic stem cells to adult liver fates. *Hepatology* **52**, 1443–1454 (2010).
49. Kubota, H. & Reid, L.M. Clonogenic hepatoblasts, common precursors for hepatocytic and biliary lineages, are lacking classical major histocompatibility complex class I antigen. *Proc. Natl. Acad. Sci. USA* **97**, 12132–12137 (2000).
50. Ma, Y., Yates, J., Liang, Y., Lemon, S.M. & Yi, M. NS3 helicase domains involved in infectious intracellular hepatitis C virus particle assembly. *J. Virol.* **82**, 7624–7639 (2008).
51. Yanagi, M., Purcell, R.H., Emerson, S.U. & Bukh, J. Transcripts from a single full-length cDNA clone of hepatitis C virus are infectious when directly transfected into the liver of a chimpanzee. *Proc. Natl. Acad. Sci. USA* **94**, 8738–8743 (1997).
52. Shimakami, T. *et al.* Stabilization of hepatitis C virus RNA by an Ago2–miR-122 complex. *Proc. Natl. Acad. Sci. USA* **109**, 941–946 (2012).
53. Date, T. *et al.* Novel cell culture-adapted genotype 2a hepatitis C virus infectious clone. *J. Virol.* **86**, 10805–10820 (2012).
54. Saeed, M. *et al.* Efficient replication of genotype 3a and 4a hepatitis C virus replicons in human hepatoma cells. *Antimicrob. Agents Chemother.* **56**, 5365–5373 (2012).
55. Timpe, J.M. *et al.* Hepatitis C virus cell-cell transmission in hepatoma cells in the presence of neutralizing antibodies. *Hepatology* **47**, 17–24 (2008).
56. Kannan, R.P., Hensley, L.L., Evers, L.E., Lemon, S.M. & McGivern, D.R. Hepatitis C virus infection causes cell cycle arrest at the level of initiation of mitosis. *J. Virol.* **85**, 7989–8001 (2011).
57. Puneet, P. *et al.* SphK1 regulates proinflammatory responses associated with endotoxin and polymicrobial sepsis. *Science* **328**, 1290–1294 (2010).
58. Dansako, H. *et al.* Class A scavenger receptor 1 (MSR1) restricts hepatitis C virus replication by mediating toll-like receptor 3 recognition of viral RNAs produced in neighboring cells. *PLoS Pathog.* **9**, e1003345 (2013).
59. Shaner, R.L. *et al.* Quantitative analysis of sphingolipids for lipidomics using triple quadrupole and quadrupole linear ion trap mass spectrometers. *J. Lipid Res.* **50**, 1692–1707 (2009).
60. Sullards, M.C., Liu, Y., Chen, Y. & Merrill, A.H. Jr. Analysis of mammalian sphingolipids by liquid chromatography tandem mass spectrometry (LC-MS/MS) and tissue imaging mass spectrometry (TIMS). *Biochim. Biophys. Acta* **1811**, 838–853 (2011).
61. Reynolds, E.S. The use of lead citrate at high pH as an electron-opaque stain in electron microscopy. *J. Cell Biol.* **17**, 208–212 (1963).
62. Papin, J.F., Vahrson, W. & Dittmer, D.P. SYBR green-based real-time quantitative PCR assay for detection of West Nile Virus circumvents false-negative results due to strain variability. *J. Clin. Microbiol.* **42**, 1511–1518 (2004).
63. Gurukumar, K.R. *et al.* Development of real time PCR for detection and quantitation of Dengue Viruses. *Virol. J.* **6**, 10 (2009).
64. Qu, L. *et al.* Disruption of TLR3 signaling due to cleavage of TRIF by the hepatitis A virus protease-polymerase processing intermediate, 3CD. *PLoS Pathog.* **7**, e1002169 (2011).
65. Ahmed, R., Salmi, A., Butler, L.D., Chiller, J.M. & Oldstone, M.B. Selection of genetic variants of lymphocytic choriomeningitis virus in spleens of persistently infected mice. Role in suppression of cytotoxic T lymphocyte response and viral persistence. *J. Exp. Med.* **160**, 521–540 (1984).
66. Bartenschlager, R., Lohmann, V. & Penin, F. The molecular and structural basis of advanced antiviral therapy for hepatitis C virus infection. *Nat. Rev. Microbiol.* **11**, 482–496 (2013).
67. Humphrey, W., Dalke, A. & Schulten, K. VMD: visual molecular dynamics. *J. Mol. Graph.* **14**, 33–38, 27–28 (1996).

JVI
Journals.ASM.org

# hnRNP L and NF90 Interact with Hepatitis C Virus 5′-Terminal Untranslated RNA and Promote Efficient Replication

You Li, Takahiro Masaki, Tetsuro Shimakami,* Stanley M. Lemon

Departments of Medicine and Microbiology Immunology, and Lineberger Comprehensive Cancer Center, The University of North Carolina at Chapel Hill, Chapel Hill, North Carolina, USA

**ABSTRACT**

**The 5′-terminal sequence of the hepatitis C virus (HCV) positive-strand RNA genome is essential for viral replication. Critical host factors, including a miR-122/Ago2 complex and poly(rC)-binding protein 2 (PCBP2), associate with this RNA segment. We used a biotinylated RNA pulldown approach to isolate host factors binding to the HCV 5′ terminal 47 nucleotides and, in addition to Ago2 and PCBP2, identified several novel proteins, including IGF2BP1, hnRNP L, DHX9, ADAR1, and NF90 (ILF3). PCBP2, IGF2BP1, and hnRNP L bound single-stranded RNA, while DHX9, ADAR1, and NF90 bound a cognate double-stranded RNA bait. PCBP2, IGF2BP1, and hnRNP L binding were blocked by preannealing the single-stranded RNA bait with miR-122, indicating that they bind the RNA in competition with miR-122. However, IGF2BP1 binding was also inhibited by high concentrations of heparin, suggesting that it bound the bait nonspecifically. Among these proteins, small interfering RNA-mediated depletion of hnRNP L and NF90 significantly impaired viral replication and reduced infectious virus yields without substantially affecting HCV internal ribosome entry site-mediated translation. hnRNP L and NF90 were found to associate with HCV RNA in infected cells and to coimmunoprecipitate with NS5A in an RNA-dependent manner. Both also associate with detergent-resistant membranes where viral replication complexes reside. We conclude that hnRNP and NF90 are important host factors for HCV replication, at least in cultured cells, and may be present in the replication complex.**

**IMPORTANCE**

**Although HCV replication has been intensively studied in many laboratories, many aspects of the viral life cycle remain obscure. Here, we use a novel RNA pulldown strategy coupled with mass spectrometry to identify host cell proteins that interact functionally with regulatory RNA elements located at the extreme 5′ end of the positive-strand RNA genome. We identify two, primarily nuclear RNA-binding proteins, hnRNP L and NF90, with previously unrecognized proviral roles in HCV replication. The data presented add to current understanding of the replication cycle of this pathogenic human virus.**

Hepatitis C virus (HCV) is a leading cause of liver disease, including chronic hepatitis, cirrhosis, and hepatocellular carcinoma. It is classified within the *Flaviviridae* family of viruses and has a single-stranded, messenger-sense RNA genome ~9.7 kb in length. The replication of HCV viral RNA is uniquely dependent on a host-factor microRNA (miRNA), miR-122, which is highly abundant in liver (1, 2). There are two conserved miR-122 binding sites (S1 and S2) located near the 5′ end of the positive-sense HCV RNA genome. Direct interactions between miR-122, and these sites are essential for the HCV life cycle (3, 4). This is reflected clinically in dose-dependent reductions of circulating HCV RNA after intravenous administration of an antisense miR-122 "antagomir" to HCV-infected chimpanzees and humans (5, 6).

Previous studies demonstrate that binding of miR-122 to the 5′-untranslated region (5′UTR) of the HCV genome stimulates viral protein expression (7, 8) and also physically stabilizes the RNA in infected cells (9, 10). Similar to conventional miRNA action, miR-122 recruits Argonaute 2 protein (Ago2) to the viral RNA (9, 11). The stability conferred by the miR-122/Ago2 complex can be substituted functionally by addition of a 5′ cap, suggesting that it protects against 5′-exonuclease-mediated decay (9). Indeed, studies of RNA decay pathways have revealed that HCV RNA is primarily degraded from the 5′ end by the exonuclease Xrn1 in infected cells and that the binding of miR-122 to the HCV 5′UTR effectively blocks Xrn1-mediated degradation (10). However, depletion of Xrn1 in Huh-7.5 cells failed to rescue the replication of HCV RNA containing single-base substitutions in both S1 and S2 that ablate miR-122 binding, suggesting that miR-122 has an additional, essential role in HCV replication beyond protecting the RNA genome from Xrn1-mediated degradation (10).

The 5′UTR of HCV folds into conserved stem-loops (SL1 to SL4), with SL2 to SL4 participating in HCV internal ribosome entry site (IRES)-directed translation (12, 13). The 5′UTR serves as a platform to recruit proteins that are essential for viral protein synthesis and RNA replication. Cellular RNA-binding proteins, including eukaryotic initiation factor 3 (eIF3), the 40S ribosomal subunit, polypyrimidine-tract-binding protein (PTB), poly(rC)-binding protein 2 (PCBP2), and La autoantigen, have been shown to bind to the 5′UTR of HCV RNA and to play important roles in viral translation and/or replication (14–18). The miR-122 binding sites (S1 and S2) are located upstream of SL2, encompassing the

Received 23 January 2014 Accepted 6 April 2014
Published ahead of print 9 April 2014
Editor: B. Williams
Address correspondence to Stanley M. Lemon, smlemon@med.unc.edu.
* Present address: Tetsuro Shimakami, Department of Gastroenterology, Kanazawa University Graduate School of Medicine, Takara-Machi, Japan.
Copyright © 2014, American Society for Microbiology. All Rights Reserved.
doi:10.1128/JVI.00225-14

SL1 region and extending to the very 5′ end of HCV RNA (Fig. 1A). This region has been shown to be essential for HCV RNA replication (14, 19). Two proteins, Ago2 and PCBP2, are known to associate with this region: Ago2 is recruited by miR-122, whereas PCBP2 has been suggested to bind to SL1, a small stem-loop near the 5′ end (9, 14, 20). In the present study, we sought to identify additional proteins associating with this region of the HCV genome, either dependently or independently of miR-122, and to assess their function in HCV replication. We found that hnRNP L and IGF2BP1 bind to single-stranded RNA (ssRNA) representing the extreme 5′ end of the HCV genome, whereas DHX9, ADAR1, and NF90 associate with the cognate double-stranded RNA (dsRNA). Among these proteins, hnRNP L and NF90 are shown to be required for efficient HCV replication but not HCV IRES-directed translation. Both proteins bind viral RNA in infected cells and may be associated with viral replication complexes.

## MATERIALS AND METHODS

**Cells, reagents, and plasmids.** Huh-7.5 cells (obtained from Charles Rice, Rockefeller University) and FT3-7 cells were maintained as described previously (8, 21). U2OS cells with conditional expression of the HCV NS5A protein were kindly provided by Darius Moradpour (Université de Lausanne) (22). WST-1 reagent (Millipore) was used to monitor cell proliferation according to the manufacturer's suggested protocol. Plasmids pH77S.3/GLuc2A and pHJ3-5 (both infectious HCV molecular clones) have been described previously (8, 23). pHCVΔC-GLuc expresses an HCV "minigenome" comprised of RNA sequence encoding the first 12 amino acids of the HCV core protein fused at its downstream end to the *Gaussia princeps* luciferase (GLuc) sequence and flanked by the 5′ and 3′ untranslated RNA sequences of H77S, a genotype 1a virus (24).

**RNA transcription.** Viral RNAs were transcribed *in vitro* as described previously (9).

**Biotinylated RNA pull-down.** Oligoribonucleotide baits, H77S 1-47 and S1/S2p6 (Fig. 1A), representing the 5′ 47 nucleotides of wild-type genotype 1 HCV RNA and a related S1/S2p6 mutant (see below) and conjugated to biotin at their 3′ ends, were synthesized by Dharmacon (Pittsburgh, PA). These RNA baits (10 pmol in each reaction) were incubated alone or with 10 pmol of a similarly synthesized complementary antisense oligonucleotide (to generate a dsRNA bait) or variable amounts of single-strand synthetic miR-122 (9), heated at 75°C for 5 min, and then cooled to room temperature. Annealed RNAs were bound to magnetic streptavidin T1 beads (Invitrogen) according to the manufacturer's instructions and then incubated with Huh-7.5 cell cytoplasmic lysate for 1 h at 4°C. Anti-miR-122 or anti-random locked nucleic acid (LNA) oligonucleotides (9) were added to the lysate where indicated. Proteins bound to the beads were eluted with SDS-PAGE sample buffer, resolved by SDS-PAGE and subjected to SYPRO Ruby staining or immunoblotting with specific antibodies. Specific bands were cut from the gel and proteins in each identified by mass spectrometry with the UNC Proteomics Core Facility.

**Transfections.** siRNA pools targeting IGF2BP1, hnRNP L, ADAR1, DHX9, NF90, and control small interfering RNA (siRNA) pools (Dharmacon) were transfected using siLentfect lipid reagent (Bio-Rad). *In vitro*-transcribed HCV RNA (1.25 μg) was transfected into $2.5 \times 10^6$ Huh-7.5 cells using the TransIT mRNA kit (Mirus Bio).

**Real-time reverse transcription-PCR (RT-PCR).** To quantify HCV RNA, cDNA was produced by reverse transcription of RNA using oligo(dT) and an HCV-specific primer (5′-GGCCAGTATCAGCACTCTC TGCAGTC-3′) targeting the 3′UTR of the genome and SuperScript III reverse transcriptase (Invitrogen). Quantitative PCR analysis was carried out using iTaq SYBR green Supermix with the CFX96 system (Bio-Rad). HCV RNA abundance was determined by reference to a standard curve using PCR primers targeting the 5′UTR (5′-CATGGCGTTAGTATGAG TGTCGT-3′ and 5′-CCCTATCAGGCAGTACCACAA-3′) and normalized to the abundance of β-actin mRNA (primers 5′-GTCACCGGAGTC CATCACG-3′ and 5′-GACCCAGATCATGTTTGAGACC-3′). The HCV minigenome RNA was amplified by the primers 5′-CACGCCCAAGATG AAGAAGT-3′ and 5′-GAACCCAGGAATCTCAGGAATG-3′.

**Immunoblots.** Immunoblotting was carried out according to standard methods with the following antibodies: mouse monoclonal antibody (MAb) to β-actin (AC-74; Sigma-Aldrich); rat MAb to Ago2 (Sigma-Aldrich); rabbit polyclonal antibodies to ADAR1, NF90, and DHX9 (Bethyl Laboratory); mouse MAb to hnRNP L (Millipore); rabbit polyclonal antibody to IGF2BP1 (Abcam); mouse MAb to PCBP2 (Abnova); mouse MAb to hnRNP C and PTB (Abcam); MAb to HCV core protein (Pierce); and rabbit polyclonal antibody to HCV NS5A protein (kindly provided by Takaji Wakita). Protein bands were visualized with an Odyssey infrared imaging system (Li-Cor Biosciences).

***Gaussia* luciferase (GLuc) assay.** Cell culture supernatant fluids were collected at intervals after RNA transfection, and cells were refed with fresh media. Secreted GLuc activity was measured in the supernatant fluids using the Biolux *Gaussia* luciferase assay kit (New England BioLabs) as previously described (23).

**Infectious virus titration.** Supernatant fluids (100 μl) from HJ3-5 virus-infected cells were incubated with $5 \times 10^4$ uninfected Huh-7.5 cells in a 48-well plate for 6 h. After replacement of media, cells were allowed to grow for 72 h before fixation and immunolabeling with anti-core antibody (Pierce). Foci of infected cells were visualized and infectious virus titer quantified in terms of focus-forming units as described previously (24).

**Preparation of cytoplasmic and nuclear lysates.** Huh-7.5 cells were harvested in lysis buffer A (150 mM KCl, 25 mM Tris-HCl [pH 7.5], 5 mM EDTA,1% Triton X-100, 2 mM dithiothreitol, Complete protease inhibitor mixture [Roche, Mannheim, Germany]). Lysates were centrifuged for 5 min at 1,000 × *g* at 4°C. The supernatants were collected as a cytoplasmic lysate. The nuclear pellet was washed with phosphate-buffered saline and lysed in buffer B (500 mM KCl, 25 mM Tris-HCl [pH 7.5], 2 mM EDTA, 1% NP-40, 0.1% SDS, Complete protease inhibitor mixture). Cytoplasmic and nuclear lysates were cleared by centrifugation at 17,000 × *g* for 10 min at 4°C.

**Immunoprecipitation.** Cytoplasmic lysates of HJ3-5 virus-infected Huh-7.5 cells were incubated with anti-hnRNP L (Millipore), anti-NF90 (Bethyl Labs), anti-Dcp1a (Abnova), rabbit anti-NS5A (kindly provided by T. Wakita), or isotype control IgG at 4°C for 2 h, followed by addition of 30 μl of protein G-Sepharose (GE Healthcare) for 1 h. RNase A was added to the lysate where indicated. The Sepharose beads were washed three times in lysis buffer. Proteins were eluted with SDS-PAGE sample buffer and subjected to SDS-PAGE, followed by immunoblotting. Coprecipitated RNAs were extracted using the RNeasy minikit (Qiagen). HCV RNA was detected by reverse transcription-PCR (RT-PCR) using the SuperScript One-Step RT-PCR (Invitrogen) and the specific primers 5′-CA TGGCGTTAGTATGAGTGTCGT-3′ and 5′-CCCTATCAGGCAGTAC CACAA-3′.

**Membrane flotation assay.** The membrane flotation assay was carried out according the method of Okamoto et al. (25) with some modifications. Eight million FT3-7 cells with or without HJ3-5 virus infection were harvested, suspended in 1 ml of TNE buffer (25 mM Tris-HCl [pH 7.4] containing 150 mM NaCl, 5 mM EDTA, and Complete protease inhibitor cocktail), and then disrupted by 20 passages through a 25-gauge needle. After low-speed centrifugation (1,000 × *g*), postnuclear supernatants were divided into two tubes and incubated for 30 min on ice with or without 0.5% Triton X-100. The lysates were mixed with 1.2 ml of an iodixanol (OptiPREP; Sigma-Aldrich, St. Louis, MO) solution with a final concentration of 45%. This mixture was overlaid with a 35 to 10% iodixanol gradient and then centrifuged at 42,000 rpm and 4°C for 14 h in an SW55 Ti rotor (Beckman Coulter, Fullerton, CA). Twelve fractions were collected from the top of the gradient and precipitated with trichloroacetic acid, followed by acetone washing. Dried pellets were resolved in the loading buffer, boiled, and subjected to SDS-PAGE, followed by immu-

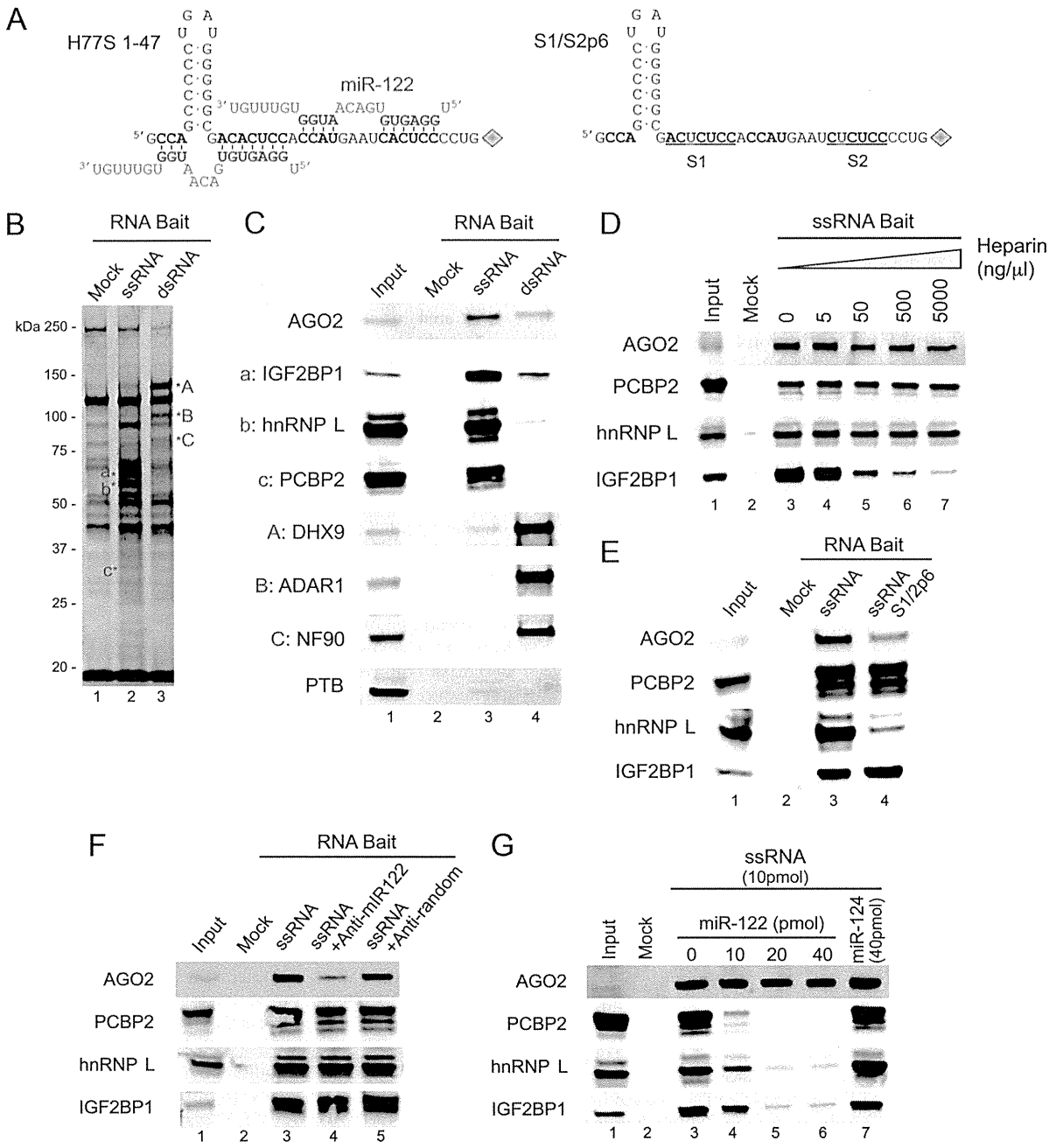


FIG 1 Identification of proteins binding to the 5′ end of the HCV 5′UTR. (A) RNA baits used in the pulldown experiments. (Left) ssRNA oligonucleotide representing the 5′ most 47 bases in the HCV genome (H77S virus, black font). Two copies of miR-122 (red font) are shown bound to the probe as determined by prior genetic studies (21). Positions involved in base-pairing are shown in boldface. (Right) S1/S2p6, a related bait with base substitutions (red font) at position 6 of the two miR-122 seed sequence binding sites, S1 and S2 (underlined). RNA probes were conjugated to biotin (diamond symbol) at their 3′ ends. (B) RNA pulldown. Synthetic biotinylated RNA bait (H77S 1-47) was incubated with Huh-7.5 cytoplasmic lysate by itself (ssRNA bait) or after being preannealed with a complementary negative-strand RNA (dsRNA bait). Proteins pulled down were resolved by SDS-PAGE and stained by SYPRO Ruby. Unique protein bands in each lane indicated by asterisks were identified by mass spectrometry. Mock, no RNA bait. (C) Protein samples from panel B were subjected to immunoblot analysis with specific antibodies. 2% input lysate was loaded as reference. Ago2, IGF2BP1, hnRNP L and PCBP2 bind preferentially to ssRNA bait, while DHX9, ADAR1, and NF90 bind to dsRNA bait. PTB was detected as a negative control. (D) RNA pulldown assay was done as in panel B using ssRNA bait in the presence of the indicated amount of heparin. Ago2, PCBP2, IGF2BP1, and hnRNP L proteins were detected by immunoblotting. Heparin inhibited the binding of IGF2BP1, but not the other proteins. (E) RNA pulldown assay was performed as in panel B using RNA bait containing single mutations in S1 and S2 site (S1/2p6, see panel A). S1/S2p6 RNA demonstrated reduced binding of Ago2 and hnRNP L but not IGF2BP1 and PCBP2. (F) RNA pulldown assay was carried out as in panel B except that anti-miR-122 or anti-random oligonucleotides were added to the lysate. Ago2, PCBP2, IGF2BP1, and hnRNP L proteins were detected by immunoblotting. Anti-miR-122 blocked the binding of Ago2 but not the other proteins. (G) RNA pulldown assay was carried out as in panel B except that 10 pmol of ssRNA bait was preannealed with the indicated amount of single-strand miR-122 or miR-124. Ago2, PCBP2, IGF2BP1, and hnRNP L proteins were detected by immunoblotting. The addition of miR-122 blocked the binding of PCBP2, IGF2BP1, and hnRNP L but not Ago2.

noblotting. Protease treatment was carried out with 1 μg of proteinase K per 50-μl fraction sample with or without 1% NP-40 and then incubated at 37°C for 30 min.

**Statistical tests.** Statistical significance was calculated using Prism 5 for Mac OS X (GraphPad Software, Inc.) and specific statistical tests as indicated.

## RESULTS

To identify proteins that bind to the 5′ terminus of positive-strand HCV RNA, we used a biotin-tagged RNA pulldown strategy. A synthetic oligonucleotide representing the 5′ 47 nucleotides of genotype 1 H77 virus was conjugated to biotin at its 3′ end (Fig. 1A, left). This RNA bait (ssRNA bait) was incubated with Huh-7.5 cell cytoplasmic lysate. Since double-strand RNA is an important intermediate in HCV RNA replication, we also sought to isolate proteins that bind to a double-stranded version of this bait by preannealing it with a complementary negative-strand RNA oligonucleotide (dsRNA bait). The proteins associated with these baits were pulled down with streptavidin beads, resolved by SDS-PAGE, and visualized by SYPRO Ruby staining (Fig. 1B). Specific bands that were pulled down by ssRNA or dsRNA bait were cut from the gel and identified by mass spectrometry. We identified three proteins that specifically associated with the ssRNA bait (Fig. 1B, lane 2, bands a, b, and c). These were identified by mass spectrometry as insulin-like growth factor 2 mRNA binding protein 1 (IGF2BP1), heterogeneous nuclear ribonucleoprotein L (hnRNP L), and PCBP2, respectively. Three bands that specifically bound the dsRNA bait (Fig. 1B, lane 3, bands A, B, and C) were found to be DEAH box helicase 9 (DHX9, also known as ATP-dependent RNA helicase 9), dsRNA-specific adenosine deaminase (ADAR1), and "nuclear factor of activated T cells 90 kDa" (NF90; also known as interleukin enhancer-binding factor 3 [ILF3]). To confirm the mass spectrometry results, we used immunoblotting with specific antibodies to these proteins. Consistently, we detected specific binding of IGF2BP1, hnRNP L, and PCBP2 to the ssRNA bait and binding of DHX9, ADAR1, and NF90 to the dsRNA bait (Fig. 1C).

As the 5′ HCV RNA sequence contains both miR-122 binding sites, we anticipated that endogenous miR-122 would bind with Ago2 protein to the ssRNA bait (9). This was confirmed in immunoblots (Fig. 1C), although Ago2 was not visible by SYPRO Ruby staining due to low abundance or inefficient binding of endogenous miR-122 to the bait. In contrast, PTB, an RNA-binding protein required for HCV replication (16), did not appear to bind either ssRNA or dsRNA bait in our assay and served as a negative control (Fig. 1C). IGF2BP1, hnRNP L, and PCBP2 are all RNA-binding proteins. PCBP2 has been shown to bind to the SLI region of the HCV 5′UTR and to be required for HCV replication (14, 20). IGF2BP1 has also been found to bind to the 5′ sequence of HCV RNA and to modulate HCV IRES function (26, 27). hnRNP L is a novel factor identified in our assay that has not been shown previously to bind the 5′ end of HCV RNA. DHX9, ADAR1, and NF90 all contain double-strand RNA-binding motifs, which is consistent with their binding to the dsRNA bait. DHX9 has RNA helicase activity, ADAR1 is an RNA specific adenosine deaminase, and NF90 was first discovered as a subunit of a nuclear transcription factor complex (28). Their function in HCV replication has not been well studied. To test the specificity of the interaction between these RNA-binding proteins and the bait, we repeated the ssRNA pulldown assay in the presence of a nonspecific competitor, heparin (Fig. 1D). Increasing amounts of heparin reduced the binding of IGF2BP1 but had little effect on the binding of Ago2, PCBP2, or hnRNP L, confirming that Ago2 (miR-122), PCBP2 and hnRNP L interact with the HCV 5′ terminal sequence in a specific and likely sequence-dependent manner.

To determine whether the binding of IGF2BP1, hnRNP L, and PCBP2 to the HCV 5′ sequence is dependent on binding of miR-122, such as Ago2 (9), we repeated the pulldown assay using a mutant RNA bait that contains a single base substitution in both the S1 and the S2 sites (Fig. 1A, right, S1/2p6) that significantly reduces miR-122 binding. As expected (9), the mutation substantially reduced Ago2 binding (Fig. 1E). Interestingly, it also diminished binding of hnRNP L but not PCBP2 or IGF2BP1 (Fig. 1E), which suggests that hnRNP L binding might be dependent on miR-122. To assess this further, we carried out a pulldown assay in the presence of an antisense anti-miR-122 locked nucleic acid (LNA) oligonucleotide. However, while the antagomir dramatically reduced Ago2 binding to the ssRNA bait, there was no effect on the binding of any of the other proteins, indicating that they bind to HCV RNA independently of miR-122 (Fig. 1F). Therefore, the reduced binding of hnRNP L to the p6 mutant RNA is unlikely to be due to reduced miR-122 binding and is more likely caused by direct disruption of the hnRNP L binding site. If this is the case, it indicates that hnRNP L binds to the same or overlapping site as the miR-122 seed sequence. Indeed, when we preannealed miR-122 to the ssRNA bait, the binding of hnRNP L was dramatically decreased in a miR-122 dose-dependent manner (Fig. 1G). Surprisingly, the binding of IGF2BP1 and PCBP2 was also blocked by miR-122. These data indicate that IGF2BP1, hnRNP L, and PCBP2 bind the HCV 5′ sequence in competition, not in cooperation with miR-122. This is not surprising given the extensive interactions of miR-122 with this segment of the viral genome (Fig. 1A, left).

We next sought to determine whether proteins that bind the 5′ end of HCV RNA have a function in HCV replication. Since Ago2 and PCBP2 have already been demonstrated to be required for HCV replication, we focused on the other proteins detected in our pulldown assay, including IGF2BP1, hnRNP L, ADAR1, DHX9, and NF90. We knocked down the expression of these proteins by transfecting specific siRNAs into Huh-7.5 cells (Fig. 2A) and then transfected a modified HCV genomic RNA that expresses *Gaussia princeps* luciferase (GLuc) as a reporter. Secreted GLuc activity was monitored over 72 h as an indicator of HCV replication (9). siRNA-mediated depletion of hnRNP L and NF90 substantially reduced HCV replication. Depletion of IGF2BP1 and DHX9 caused much smaller but nonetheless reproducible and statistically significant reductions in replication, while ADAR depletion was without effect (Fig. 2B). These results suggested that, among these RNA-binding proteins, hnRNP L and NF90 may be particularly important for efficient HCV replication. However, depletion of either protein also caused significant defects in cell proliferation as measured by WST-1 assay, in both cases reducing cell growth by ca. 25% (Fig. 2C).

Further studies focused on hnRNP L and NF90. To minimize the impact of their depletion on cell growth, we repeated the RNA interference experiments in cells cultured in media containing 2% serum (Fig. 3). HCV replication was significantly reduced by depletion of either protein, as measured by GLuc activity (Fig. 3A). Total HCV RNA abundance was also reduced by ca. 60%, after hnRNP L depletion and 40% after NF90 depletion (Fig. 3B). Importantly, hnRNP L and NF90 depletion resulted in little change

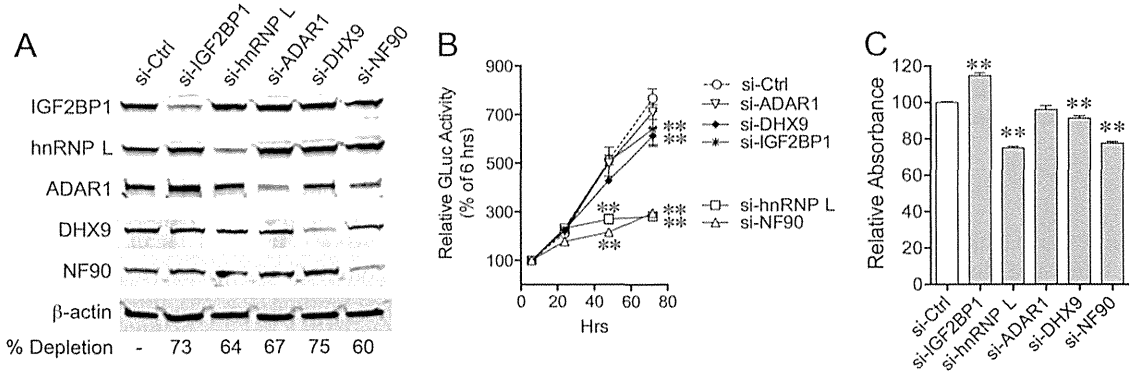


**FIG 2** Depletion of hnRNP L or NF90 impairs HCV replication. Huh-7.5 cells were transfected with siRNAs targeting the indicated proteins or scrambled si-Ctrl and then 48 h later retransfected with H77S.3/GLuc2A RNA. (A) Immunoblots of IGF2BP1, hnRNP L, ADAR1, DHX9, and NF90 72 h after siRNA transfection. β-Actin was included as a loading control. The percent depletion of each protein is shown. (B) Relative GLuc activity in supernatant fluids from Huh-7.5 cells transfected with HCV RNA and the indicated siRNAs. The results shown represent the means of three replicate experiments ± the standard deviations. Values at 6 h were arbitrarily set to 100. **, $P < 0.01$ (compared to si-Ctrl by two-way analysis of variance [ANOVA]). (C) WST-1 assay measurement of proliferation of cells transfected with indicated siRNAs at 72 h after HCV RNA transfection. Values for control siRNA were arbitrarily set to 100. **, $P < 0.01$(compared to si-Ctrl by two-way ANOVA with Bonferroni's multiple-comparison test.)

in cell proliferation (Fig. 3C). We confirmed these results by infecting Huh-7.5 cells with HJ3-5 virus, an HCV genotype 1a/2a chimera that efficiently replicates and produces infectious particles in cell culture. Knockdown of hnRNP L dramatically diminished HJ3-5 replication, as measured by expression of HCV core and NS5A proteins; knockdown of NF90 also modestly reduced the abundance of core and NS5A proteins (Fig. 3D). Consistently, hnRNP L and NF90 knockdown resulted in 3- and 1.5-fold reductions in infectious virus yield after 72 h compared to cells transfected with a nontargeting control siRNA (Fig. 3E). The above-described experiments used siRNA pools targeting hnRNP L and NF90. To assess the possibility that inhibition of replication resulted from off-target effects of these siRNAs, we compared the knockdown efficiency of individual siRNAs with their impact on viral replication. We observed substantial variation in the capacity of individual siRNAs to deplete hnRNP L or NF90 (Fig. 3F), but with both proteins the degree of depletion strongly correlated with the magnitude of the reduction in HCV replication, as measured by GLuc assay (Fig. 3G). Thus, the reduction of HCV replication was likely caused by specific depletion of hnRNP L and NF90 and not spurious off-target effects of the siRNA. Collectively, these data strongly suggest a role for hnRNP L and NF90 in efficient HCV genome amplification.

To examine whether hnRNP L and NF90 are required for HCV IRES-mediated translation, we transfected cells with an HCV minigenome RNA comprised of the HCV 5′UTR and 3′UTR flanking the GLuc sequence as reporter (Fig. 4A). This RNA was transfected into Huh-7.5 cells depleted of hnRNP L and NF90, and secreted GLuc activity was measured over the ensuring 24 h. Depletion of hnRNP L and NF90 resulted in little difference in GLuc activity (Fig. 4B) or GLuc mRNA abundance at 24 h (Fig. 4C). These data suggest that hnRNP L and NF90 are not essential for HCV IRES-mediated translation and that they do not significantly influence the stability of RNAs containing the HCV 5′UTR. Since hnRNP L binds to the 5′ end of HCV RNA in competition with miR-122 (Fig. 1F), while NF90 binds nearby, we also tested whether hnRNP L and NF90 depletion would affect the capacity of miR-122 to promote HCV replication. We transfected H77S.3/GLuc2A RNA into control, hnRNP L- or NF90-depleted cells, together with miR-122 or miR-124. Consistent with previous reports (9, 10), miR-122 supplementation resulted in an ~2-fold increase in GLuc activity compared to a control miRNA, miR-124 (Fig. 4D). The fold increase in GLuc activity caused by miR-122 supplementation (2.06) was unchanged in hnRNP L- and NF90-depleted cells (1.95 to 2.06, Fig. 4D), indicating that significant reductions in hnRNP L and NF90 abundance do not influence miR-122 enhancement of HCV replication.

hnRNP L and NF90 have been reported to be nuclear proteins (29–31). We confirmed this by laser-scanning confocal fluorescence microscopy (data not shown). However, since the HCV life cycle is restricted to the cytoplasm, we further analyzed the distribution of hnRNP L and NF90 in Huh-7.5 cells by cytoplasmic-nuclear fractionation. As shown in Fig. 5A, hnRNP L was largely localized to the nuclear fraction, and yet a small proportion of it was present in cytoplasm. Approximately half of the NF90 abundance localized to the cytoplasm, while NF110, an isoform of NF90, was predominantly detected in the nuclear fraction. NF90 and NF110 share antigenic specificity, and this likely explains the discrepant microscopy findings. HCV infection did not alter the intracellular distribution of hnRNP L or NF90 (Fig. 5A, right).

To determine whether hnRNP L and NF90 bind to HCV RNA in infected cells, as they do *in vitro* (Fig. 1), we immunoprecipitated hnRNP L and NF90 from HJ3-5 virus-infected Huh-7.5 cells and examined the precipitate for the presence of viral RNA. hnRNP L and NF90 were efficiently pulled down by specific antibodies compared to an isotype control IgG (Fig. 5B). RNA coprecipitating with hnRNP L and NF90 was purified and HCV RNA amplified and detected by RT-PCR. As shown in Fig. 5B, HCV RNA coprecipitated with both hnRNP L and NF90, indicating that hnRNP L and NF90 associate with HCV RNA within infected cells. In contrast, antibody to Dcp1a, an mRNA-decapping protein that does not colocalize with HCV RNA in cells (10), did not pull down HCV RNA. hnRNP L and NF90 were also found to coprecipitate with NS5A in HCV-infected cells by immunoblot assay (Fig. 5C). This association was RNA dependent since RNase treatment completely abolished the interaction (Fig. 5C). To determine whether the RNA mediating the interaction between NS5A and hnRNP L or NF90 is HCV specific, we repeated this

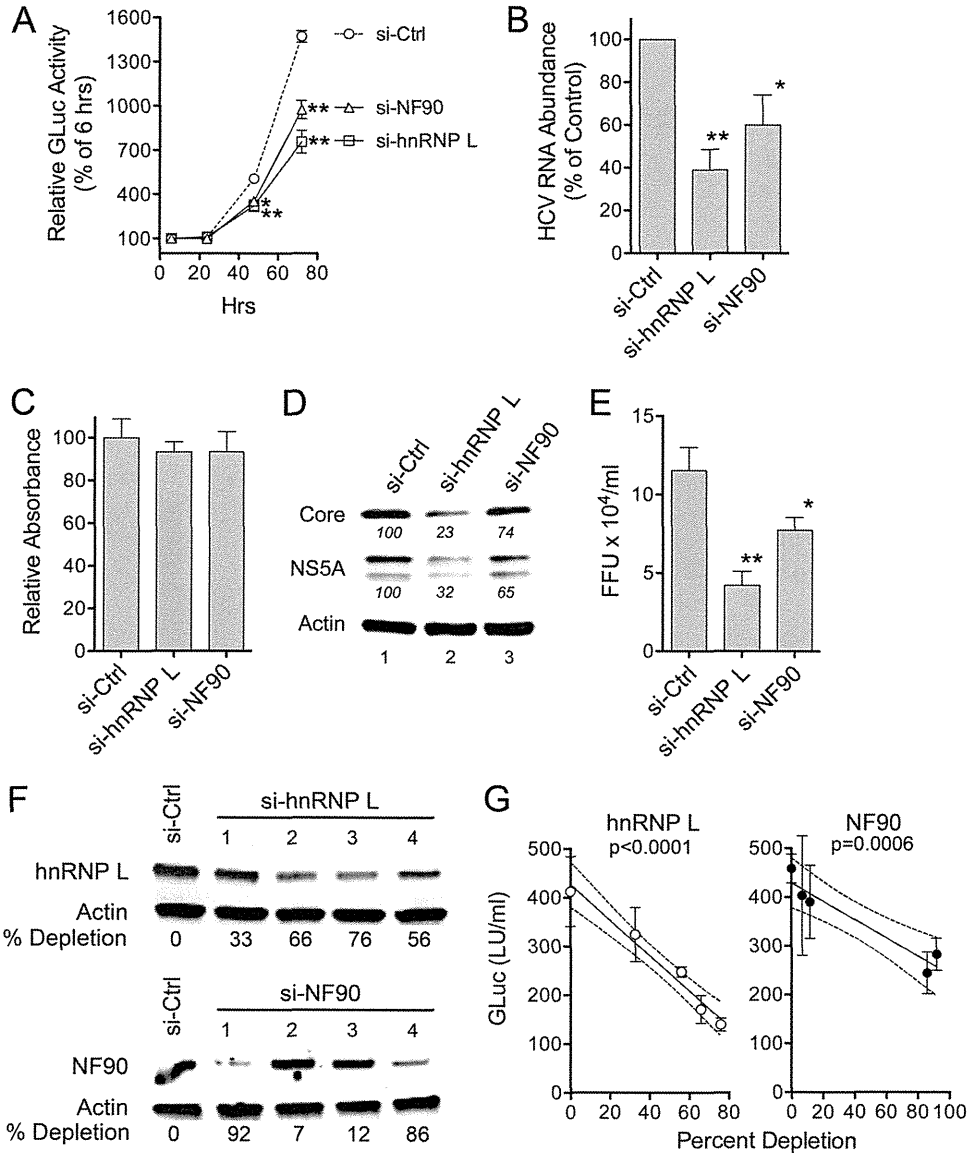


**FIG 3** hnRNP L and NF90 are required for efficient HCV replication. (A) Huh-7.5 cells were maintained in growth media containing 2% serum, and transfected with siRNAs for hnRNP L, NF90, or scrambled si-Ctrl and then 48 h later retransfected with H77S.3/GLuc2A RNA. Supernatant fluids were removed at intervals and assayed for GLuc activity. Values at 6 h were arbitrarily set to 100. The results shown represent the means of three replicate experiments ± the standard errors of the mean. *, $P < 0.05$; **, $P < 0.01$ (compared to si-Ctrl by two-way ANOVA). (B) HCV RNA was quantified relative to β-actin mRNA by real-time RT-PCR 72 h after HCV RNA transfection. *, $P < 0.05$; **, $P < 0.01$ (compared to si-Ctrl by one-way ANOVA with Bonferroni's correction for multiple comparisons). (C) WST-1 assay for measurement of proliferation of cells at 72 h after HCV RNA transfection. Values for control siRNA were arbitrarily set to 100. Values do not differ significantly from si-CTRL (one-way ANOVA with Bonferroni's post test). (D) Immunoblots of HCV core and NS5A proteins at 72 h postinfection, with β-actin as a loading control. Huh-7.5 cells were maintained in growth medium containing 2% serum and transfected with siRNAs for hnRNP L, NF90, or scrambled si-Ctrl and then 48 h later infected with HJ3-5 virus. Italicized labels show quantification of core and NS5A proteins relative to β-actin, with values for si-Ctrl arbitrarily set to 100. (E) The infectious virus titers of supernatant fluids from panel D were determined by a fluorescent focus formation assay. The results shown represent the means of three replicate experiments ± the standard deviations. *, $P < 0.05$; **, $P < 0.01$ (compared to si-Ctrl by one-way ANOVA with Bonferroni's post test). (F) Individual siRNAs targeting hnRNP L or NF90 (four each) were transfected into cells, and hnRNP L and NF90 protein abundance was determined by immunoblotting 96 h later. β-Actin was included as a loading control. hnRNP L and NF90 levels were normalized to β-actin, and the percent depletion compared to si-Ctrl was calculated for each siRNA. (G) H77S.3/GLuc2A RNA was transfected into the hnRNP L- and NF90-depleted cells shown in panel F, and GLuc activity secreted from the cells between 48 and 72 h was assessed. The results shown represent mean GLuc ± the standard deviations in three replicate cultures, plotted against the percent depletion of target protein. Dashed lines represent the outer limits of the 95% confidence-interval band for a best-fit plot. The *P* values indicate the likelihood that the slope of this line diverges from "0". Inhibition of HCV replication was highly correlated with the degree of depletion of hnRNP L and NF90.

assay using U2OS cells that conditionally express only the NS5A protein (Fig. 5D). Little interaction was evident between NS5A and hnRNP L or NF90 under these conditions (Fig. 5E), suggesting that the coprecipitation of hnRNP L and NF90 with NS5A in infected cells may be largely mediated by HCV RNA. We found no evidence that either protein directly interacts with NS5A.

Previous studies indicate that HCV RNA replication complexes are localized to detergent-resistant intracellular mem-

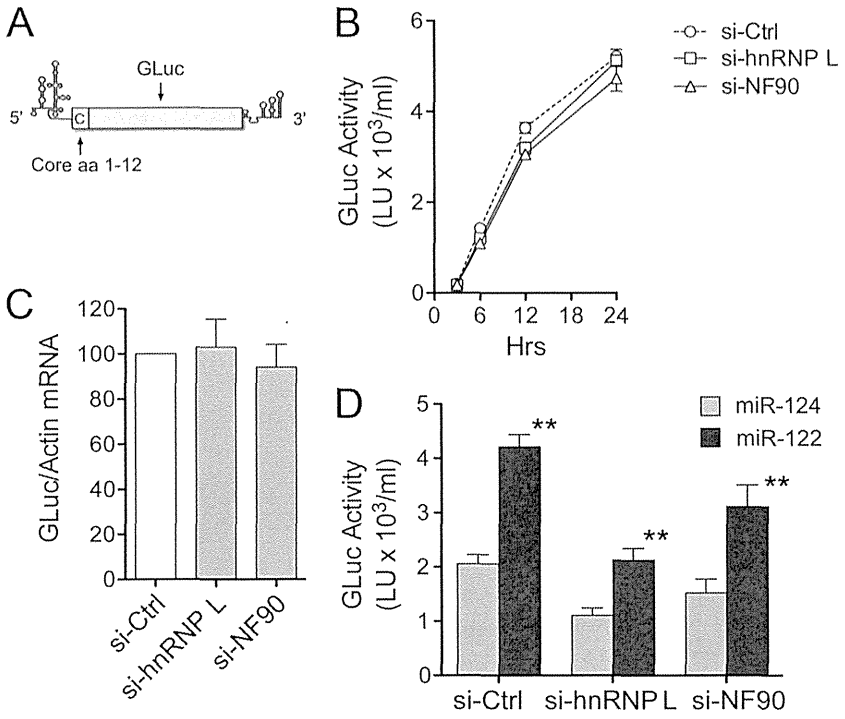


**FIG 4** hnRNP L and NF90 depletion do not affect HCV IRES translation or miR-122 enhancement of HCV replication. (A) Diagram of the HCV minigenome RNA comprising the HCV 5′UTR followed by N-terminal core protein sequence fused to GLuc and the HCV 3′ UTR. (B) Huh-7.5 cells were transfected with siRNAs for hnRNP L, NF90 or scrambled si-Ctrl, and then 48 h later retransfected with HCV minigenome RNA. GLuc activity in supernatant fluids was measured at indicated times. The results shown represent the means of three replicate experiments ± the standard deviations. Values at 3 h were arbitrarily set to 100. (C) GLuc RNA levels were determined by real-time RT-PCR 24 h after HCV minigenome RNA transfection relative to β-actin mRNA. The differences in GLuc activity between hnRNP L- and NF90-depleted cells and cells transfected with si-Ctrl at 24 h (see panel B) were not significant when normalized to mRNA abundance ($P > 0.05$ as determined by two-sided $t$ test). (D) Huh-7.5 cells were transfected with siRNAs for hnRNP L, NF90, or scrambled si-Ctrl and then 48 h later retransfected with H77s-GLuc RNA, together with 100 nM duplex miR-122 or miR-124. The GLuc activities were measured 72 h later. The results shown represent the means of three replicate experiments ± the standard deviations. **, $P < 0.01$ (compared to miR-124 by two-sided $t$ test).

branes (DRMs) (32). Thus, to examine the possibility that hnRNP L and NF90 might be associated with replication complexes, we investigated their distribution within membrane fractions recovered from a flotation gradient. Cytoplasmic membranes from uninfected or HJ3-5 virus-infected Huh-7.5 cells were treated with Triton X-100, overlaid with a density gradient, and subjected to centrifugation (see Methods). Partitioning of DRMs and detergent soluble membranes (DSM) into separate fractions was confirmed by distinct distributions of caveolin-2 and calrecticulin among these fractions (Fig. 6A). HCV replication complexes were largely associated with the DRM, as shown by the distribution of NS5A. Although hnRNP L and NF90 were readily detected in DRM fractions from uninfected cells (3.0 to 6.85% and 2.2 to 3.2% of the total of hnRNP L and NF90, respectively, in the gradient were present in fractions 1 to 4), HCV infection increased the proportion of the proteins associating with the DRM (10.0 to 21.9% hnRNP L and 12.7 to 27.6% NF90 in replicate experiments) (Fig. 6A and B). In contrast, IGF2BP1, which binds nonspecifically to our RNA bait (Fig. 1D) and the depletion of which had relatively little effect on HCV replication (Fig. 2B), was barely detectable in DRM fractions, and its distribution was not altered by HCV infection (Fig. 6A). These data indicate that HCV infection results in an increased association of hnRNP L and NF90 with DRMs, providing additional evidence that these proteins are likely to be associated with the replication complex.

To further confirm this association, we treated the DRM fractions with proteinase K. Proteins present within membranous vesicles within the DRM fraction should be resistant to proteases in the absence of strong detergents. hnRNP L and NF90 in DRM fractions from uninfected cells were completely digested by proteinase K (Fig. 6C), indicating that they are not protected by membranes. In contrast, a significant fraction of hnRNP L and NF90 in DRM fractions from HCV-infected cells was resistant to protease treatment (Fig. 6C). Pretreatment of these fractions with 1% NP-40, which should disrupt all membrane structures, rendered these proteins sensitive to proteinase K. Taken together with the increased distribution of hnRNP L and NF90 into the DRM fractions (Fig. 6A and B), these data suggest that hnRNP L and NF90 are recruited into replication complexes to facilitate replication.

## DISCUSSION

The 5′-terminal sequence of the HCV genome contains two miR-122 binding sites and is known to have an important regulatory role in viral RNA replication (3, 4, 19). The predicted secondary structure of the 47-nucleotide terminal sequence contains a conserved stem-loop (SLI), followed by an unstructured region within which the miR-122 seed sequence-binding sites are located (Fig. 1A, left). We hypothesized that these conserved regions may interact with host proteins that regulate viral RNA translation and/or replication. To assess this hypothesis, we used a biotin-RNA pulldown strategy to identify proteins that bind to this 5′-terminal sequence. In addition to Ago2 and PCBP2, which have

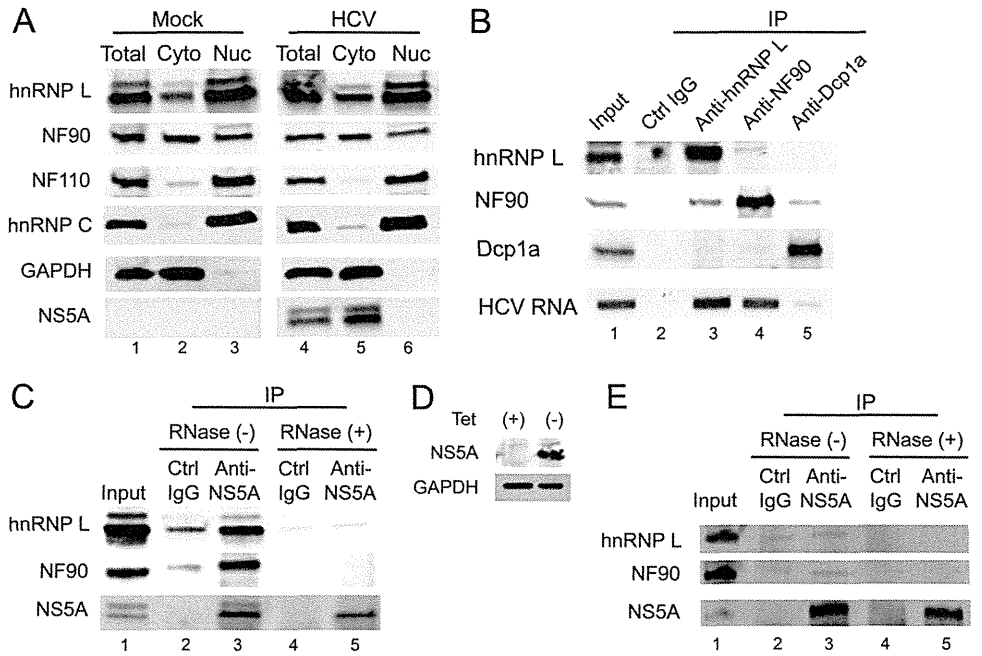


**FIG 5** Cellular localization and association of hnRNP L and NF90 with HCV RNA and NS5A. (A) Distribution of hnRNP L and NF90 in cytoplasmic and nuclear fractions. Total lysate and cytoplasmic and nuclear fractions of Huh-7.5 cells with or without HCV infection were prepared, and the distribution of the indicated proteins was assessed using immunoblotting. hnRNP L was largely localized to the nuclear fraction, with a small amount in the cytoplasm. NF90 protein was equally distributed between cytoplasmic and nuclear fractions, while NF110, an isoform of NF90, predominantly localized to the nucleus. GAPDH (glyceraldehyde-3-phosphate dehydrogenase) was used as cytoplasmic marker and hnRNP C as a nuclear marker. HCV NS5A protein was detected only in the cytoplasmic fraction from infected cells. (B) hnRNP L and NF90 associate with HCV RNA in infected cells. hnRNP L or NF90 proteins were immunoprecipitated by specific antibodies from a cytoplasmic lysate of Huh-7.5 cells infected with HJ3-5 virus. Precipitation of hnRNP L and NF90 proteins was confirmed by immunoblotting. RNAs were extracted from the precipitates, and HCV RNA was detected by RT-PCR. Isotype control IgG was used as negative control. 5% input lysate was loaded as a reference. (C) RNA-dependent association of NS5A with hnRNP L and NF90. NS5A protein was immunoprecipitated by specific antibody or control IgG from HJ3-5 virus-infected Huh-7.5 cytoplasmic lysate with or without RNase treatment. NS5A, hnRNP L, and NF90 proteins in the precipitates were detected by immunoblotting. 5% input lysate was loaded as reference. hnRNP L and NF90 coimmunoprecipitate with NS5A only in non-RNase-treated samples. (D) U2OS cells with tet-regulated expression of NS5A protein were treated with or without 2 μg of tetracycline/ml for 48 h, and the expression of NS5A was detected by immunoblotting with GAPDH as a loading control. (F) NS5A immunoprecipitation was carried out as in panel C for U2OS cells expressing NS5A protein. Little coprecipitation of hnRNP L and NF90 with NS5A was observed.

been shown previously to bind this region of the genome (9, 14, 20), we documented the binding of several novel proteins, including hnRNP L, DHX9, ADAR1, and NF90 (Fig. 1B and C). hnRNP L binds ssRNA, whereas DHX9, ADAR1, and NF90 bind the double-strand complement of this RNA segment. Among these proteins, siRNA-mediated knockdowns of either hnRNP L or NF90 reduced HCV RNA and protein levels within infected cells (Fig. 3), suggesting that both are required for efficient HCV replication. hnRNP L and NF90 function in the HCV life cycle independently of miR-122, because depletion of either did not affect the capacity of miR-122 to stimulate HCV replication (Fig. 4D). hnRNP L and NF90 depletion had no impact on GLuc activity expressed by an HCV minigenome (Fig. 4B), suggesting they are not required for HCV IRES-mediated translation.

Previous studies have demonstrated that HCV RNA replication complexes consist of viral and host proteins assembled on DRMs (32). The localization of hnRNP L and NF90 to the DRM fractions of HCV-infected cells (Fig. 6A and B) thus suggests that they may be associated with the RNA replication complex. The fact that both proteins are protected by membranes from protease digestion in these DRM fractions provides further support for this (Fig. 6C). Immunoprecipitation of hnRNP L and NF90 in HCV-infected cells confirmed their association with HCV RNA (Fig. 5B). It is particularly interesting that hnRNP L and NF90 coimmunoprecipitated with NS5A (Fig. 5C), an essential component of the replication complex. The interaction was dependent on RNA, suggesting that while hnRNP L and NF90 do not physically interact with NS5A, they may form an RNA-protein complex together, possibly in association with HCV RNA in the replication complex.

hnRNPs are proteins that interact with heterogeneous nuclear RNAs (hnRNAs) (33). Several functions have been suggested for hnRNPs, including pre-mRNA processing, mRNA translocation from the nucleus to the cytoplasm, and translation (33). This group of RNA-binding proteins has been shown to participate in both viral IRES mediated-translation and viral replication. For example, PTB (hnRNP I) has been shown to enhance IRES-dependent translation of encephalomyocarditis virus and foot-and-mouth disease virus, both picornaviruses, as well as HCV (16, 34, 35). PCBP2 (hnRNP E2) is required for efficient translation and replication of both poliovirus and HCV RNA (14, 36). hnRNP L has been reported to be localized mainly in the nucleus (29). However, we detected hnRNP L in the cytoplasm both in the presence and in the absence of HCV infection (Fig. 5), suggesting that it may shuttle between the nucleus and cytoplasm. hnRNP L was previously reported to be required for HCV IRES-dependent translation because an RNA aptamer specific for hnRNP L blocked reporter protein translation directed by the HCV IRES

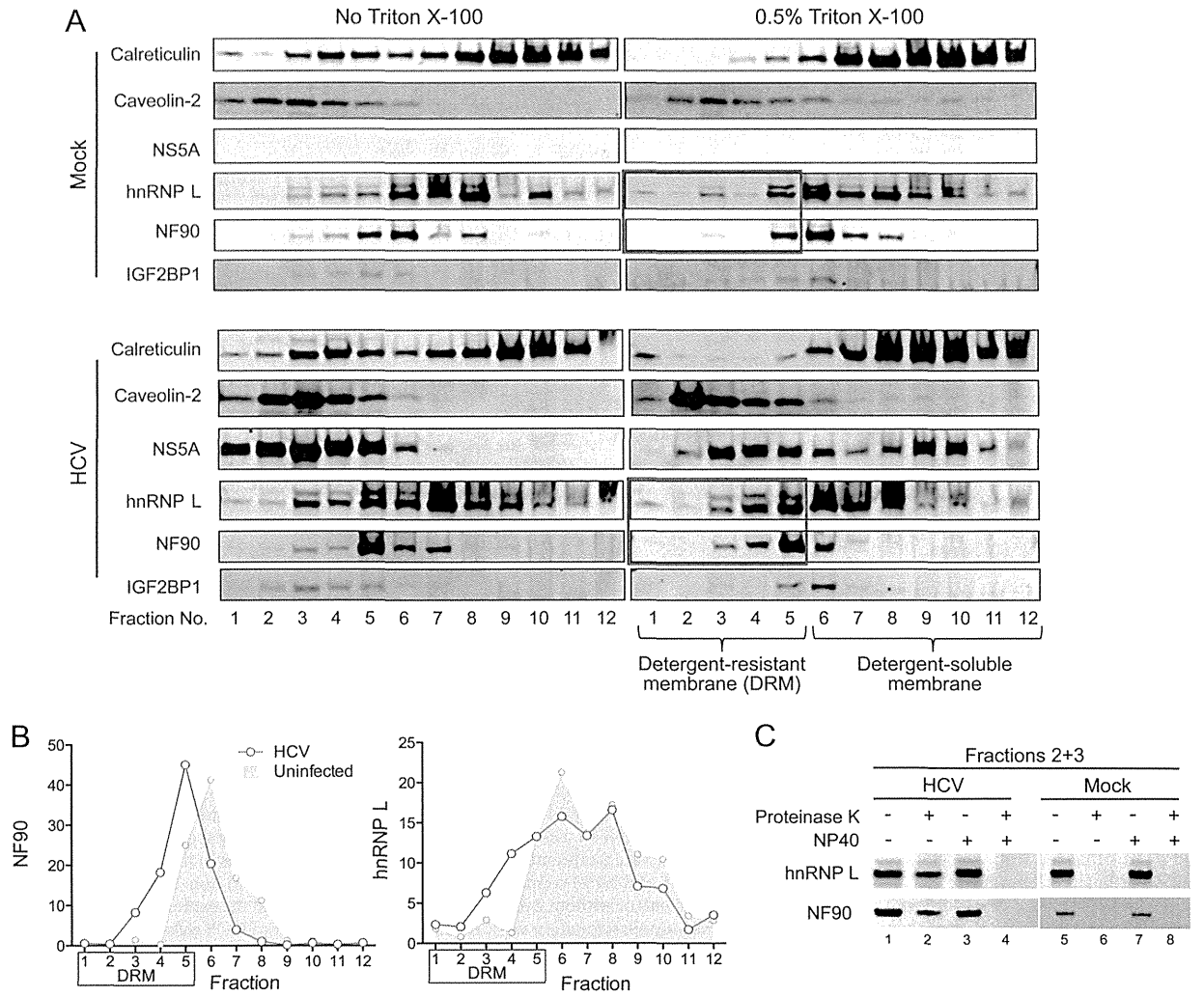


FIG 6 Membrane flotation assay. (A) Analysis of the distribution of hnRNP L and NF90 in fractions recovered from a membrane flotation assay. Cytoplasmic membranes extracted from FT3-7 cells with or without HCV infection were treated or not treated with Triton X-100, overlaid with a density gradient, and subjected to centrifugation. Fractions were subsequently recovered from the top of the gradient, and proteins in each were precipitated, resolved by SDS-PAGE, and analyzed by immunoblotting. Calrecticulin and caveolin-2 were detected as markers for detergent-soluble membrane (DSM) and detergent-resistant membrane (DRM), respectively. A substantial proportion of NS5A was located in DRM fractions, consistent with its presence in the HCV replication complex. hnRNP L and NF90 were readily detected in DRM, while little IGF2BP1 protein was found present in DRM. The image shown is representative of replicate experiments. (B) Quantification of the distribution of hnRNP L and NF90 proteins in fractions from the flotation gradients shown in panel A. Protein bands in immunoblots of each fraction were quantified with an Odyssey infrared imaging system. (C) hnRNP L and NF90 distributed to the DRM are protected from protease digestion in gradients loaded with material from HCV-infected cells. Fractions 2 and 3 (no Triton X-100) from panel A were treated with proteinase K with or without prior treatment with 1% NP-40. hnRNP L and NF90 proteins were detected by immunoblotting. hnRNP L and NF90 were uniformly sensitive to protease K in uninfected cells, whereas hnRNP L and NF90 associating with the DRM were resistant to proteinase K in HCV-infected cells. All proteins in fractions 8 and 9 from either uninfected or infected cells were sensitive to protease treatment (data not shown).

(37). However, in our study hnRNP L had little effect on the translation of a minigenome reporter containing both HCV UTRs, indicating that it is not essential for HCV IRES-dependent translation initiation (Fig. 4). It is possible the aptamer used in the previous report caused a nonspecific inhibition of IRES activity.

It is intriguing that the hnRNP L protein binding site appears to overlap with miR-122 binding sites in HCV 5′UTR, since the p6 mutation in the S1 and S2 sites reduced hnRNP L binding to the RNA bait in the pulldown experiments (Fig. 1E). However, the binding of hnRNP L to the HCV 5′ terminus is independent of miR-122, since the anti-miR-122 antagomir did not block binding of hnRNP L (Fig. 1F). In contrast, preincubation of the RNA bait with miR-122 diminished hnRNP L binding, indicating that hnRNP L and miR-122 bind competitively to overlapping sites. It is puzzling why two proviral factors, miR-122 and hnRNP L, would compete with each other. One plausible explanation is that hnRNP L and miR-122 are involved in different stages of the HCV life cycle and that a change of binding factors at the 5′ RNA terminus is accompanied by a transition between these different stages. Further work will be required to investigate this hypothesis.

NF90 belongs to a family of proteins that contain a double-strand RNA binding motif and exert a variety of functions involving RNA recognition, RNA processing, and RNA stability (38). NF90 has previously been reported to form a complex with DHX9

(39). Although DHX9 and NF90 both bound to the dsRNA bait (Fig. 1), depletion of NF90 had a much greater impact on HCV replication (Fig. 2B). NF90 has been shown to positively regulate replication of several positive-strand RNA virus, including dengue virus and bovine viral diarrhea virus, a pestivirus closely related to HCV (40, 41). This suggests its host factor function may be conserved among the *Flaviviridae*. It binds to the 5′UTRs and/or 3′UTRs of these viruses and promotes their replication. It has also been reported to associate with both the 5′UTRs and 3′UTRs of HCV in a cross-linking assay and to promote interactions between the 5′ and 3′ ends of the genome (42). Although we found that NF90 bound to the dsRNA bait (Fig. 1) and was required for efficient HCV replication (Fig. 3), we do not know whether NF90 mediates HCV replication through its direct association with dsRNA (as we have demonstrated) or by binding to structured elements within the HCV 5′UTRs and 3′UTRs. Nevertheless, the increased distribution of NF90 into DRM following HCV infection (Fig. 6) suggests the association of NF90 with viral replicase complexes.

How hnRNP L and NF90 function in HCV replication remains to be determined. The binding of hnRNP L or NF90 could facilitate replication complex assembly by recruiting other viral and host factors onto HCV RNA or possibly induce conformational changes in the RNA that promote viral RNA synthesis. Further studies are needed to dissect the individual steps in the viral life cycle impacted by hnRNP L and NF90 and to identify other host and viral proteins involved. Further elucidation of the molecular basis of the function of hnRNP L and NF90 on HCV replication could yield important insight into unrecognized actions of RNA-binding proteins in the viral life cycle and possibly provide clues for development of broadly acting antiviral therapies.

## ACKNOWLEDGMENTS

This study was supported in part by National Institutes of Health grants R01-AI095690 and R01-CA164029. Additional support was provided by the Lineberger Comprehensive Cancer Center (P30-CA16086) and the University Cancer Research Fund of the University of North Carolina.

We thank Takaji Wakita for the gift of rabbit antibody to NS5A, Darius Moradpour for the gift of cells with Tet-regulated expression of NS5A, and the staff of the UNC Proteomics Core Facility for their assistance with mass spectrometry.

## REFERENCES

1. **Chang J, Nicolas E, Marks D, Sander C, Lerro A, Buendia MA, Xu C, Mason WS, Moloshok T, Bort R, Zaret KS, Taylor JM.** 2004. miR-122, a mammalian liver-specific microRNA, is processed from hcr mRNA and may downregulate the high-affinity cationic amino acid transporter CAT-1. RNA Biol. **1**:106–113. http://dx.doi.org/10.4161/rna.1.2.1066.
2. **Jopling CL, Yi M, Lancaster AM, Lemon SM, Sarnow P.** 2005. Modulation of hepatitis C virus RNA abundance by a liver-specific microRNA. Science **309**:1577–1581. http://dx.doi.org/10.1126/science.1113329.
3. **Jopling CL, Schütz S, Sarnow P.** 2008. Position-dependent function for a tandem microRNA miR-122-binding site located in the hepatitis C virus RNA genome. Cell Host Microbe **4**:77–85. http://dx.doi.org/10.1016/j.chom.2008.05.013.
4. **Jangra RK, Yi M, Lemon SM.** 2010. miR-122 regulation of hepatitis C virus translation and infectious virus production. J. Virol. **84**:6615–6625. http://dx.doi.org/10.1128/JVI.00417-10.
5. **Janssen HL, Reesink HW, Lawitz EJ, Zeuzem S, Rodriguez-Torres M, Patel K, van der Meer AJ, Patick AK, Chen A, Zhou Y, Persson R, King BD, Kauppinen S, Levin AA, Hodges MR.** 2013. Treatment of HCV infection by targeting microRNA. N. Engl. J. Med. **368**:1685–1694. http://dx.doi.org/10.1056/NEJMoa1209026.
6. **Lanford RE, Hildebrandt-Eriksen ES, Petri A, Persson R, Lindow M, Munk ME, Kauppinen S, Orum H.** 2010. Therapeutic silencing of microRNA-122 in primates with chronic hepatitis C virus infection. Science **327**:198–201. http://dx.doi.org/10.1126/science.1178178.
7. **Henke JI, Goergen D, Zheng J, Song Y, Schuttler CG, Fehr C, Junemann C, Niepmann M.** 2008. microRNA-122 stimulates translation of hepatitis C virus RNA. EMBO J. **27**:3300–3310. http://dx.doi.org/10.1038/emboj.2008.244.
8. **Jangra RK, Yi M, Lemon SM.** 2010. Regulation of hepatitis C virus translation and infectious virus production by the microRNA miR-122. J. Virol. **84**:6615–6625. http://dx.doi.org/10.1128/JVI.00417-10.
9. **Shimakami T, Yamane D, Jangra RK, Kempf BJ, Spaniel C, Barton DJ, Lemon SM.** 2012. Stabilization of hepatitis C RNA by an Ago2-miR-122 complex. Proc. Natl. Acad. Sci. U. S. A. **109**:941–946. http://dx.doi.org/10.1073/pnas.1112263109.
10. **Li Y, Masaki T, Yamane D, McGivern DR, Lemon SM.** 2013. Competing and noncompeting activities of miR-122 and the 5′ exonuclease Xrn1 in regulation of hepatitis C virus replication. Proc. Natl. Acad. Sci. U. S. A. **110**:1881–1886. http://dx.doi.org/10.1073/pnas.1213515110.
11. **Conrad KD, Giering F, Erfurth C, Neumann A, Fehr C, Meister G, Niepmann M.** 2013. microRNA-122-dependent binding of Ago2 protein to hepatitis C virus RNA Is associated with enhanced RNA stability and translation stimulation. PLoS One **8**:e56272. http://dx.doi.org/10.1371/journal.pone.0056272.
12. **Fraser CS, Doudna JA.** 2007. Structural and mechanistic insights into hepatitis C viral translation initiation. Nat. Rev. Microbiol. **5**:29–38. http://dx.doi.org/10.1038/nrmicro1558.
13. **Honda M, Beard MR, Ping LH, Lemon SM.** 1999. A phylogenetically conserved stem-loop structure at the 5′ border of the internal ribosome entry site of hepatitis C virus is required for cap-independent viral translation. J. Virol. **73**:1165–1174.
14. **Wang L, Jeng KS, Lai MM.** 2011. Poly(C)-binding protein 2 interacts with sequences required for viral replication in the hepatitis C virus (HCV) 5′ untranslated region and directs HCV RNA replication through circularizing the viral genome. J. Virol. **85**:7954–7964. http://dx.doi.org/10.1128/JVI.00339-11.
15. **Ali N, Siddiqui A.** 1997. The La antigen binds 5′ noncoding region of the hepatitis C virus RNA in the context of the initiator AUG codon and stimulates internal ribosome entry site-mediated translation. Proc. Natl. Acad. Sci. U. S. A. **94**:2249–2254. http://dx.doi.org/10.1073/pnas.94.6.2249.
16. **Ali N, Siddiqui A.** 1995. Interaction of polypyrimidine tract-binding protein with the 5′ noncoding region of the hepatitis C virus RNA genome and its functional requirement in internal initiation of translation. J. Virol. **69**:6367–6375.
17. **Buratti E, Tisminetzky S, Zotti M, Baralle FE.** 1998. Functional analysis of the interaction between HCV 5′UTR and putative subunits of eukaryotic translation initiation factor eIF3. Nucleic Acids Res. **26**:3179–187. http://dx.doi.org/10.1093/nar/26.13.3179.
18. **Sizova DV, Kolupaeva VG, Pestova TV, Shatsky IN, Hellen CU.** 1998. Specific interaction of eukaryotic translation initiation factor 3 with the 5′ nontranslated regions of hepatitis C virus and classical swine fever virus RNAs. J. Virol. **72**:4775–4782.
19. **Friebe P, Lohmann V, Krieger N, Bartenschlager R.** 2001. Sequences in the 5′ nontranslated region of hepatitis C virus required for RNA replication. J. Virol. **75**:12047–12057. http://dx.doi.org/10.1128/JVI.75.24.12047-12057.2001.
20. **Fukushi S, Okada M, Kageyama T, Hoshino FB, Nagai K, Katayama K.** 2001. Interaction of poly(rC)-binding protein 2 with the 5′-terminal stem-loop of the hepatitis C-virus genome. Virus Res. **73**:67–79. http://dx.doi.org/10.1016/S0168-1702(00)00228-8.
21. **Shimakami T, Yamane D, Welsch C, Hensley L, Jangra RK, Lemon SM.** 2012. Base pairing between hepatitis C Virus RNA and microRNA 122 3′ of its seed sequence is essential for genome stabilization and production of infectious virus. J. Virol. **86**:7372–7383. http://dx.doi.org/10.1128/JVI.00513-12.
22. **Moradpour D, Kary P, Rice CM, Blum HE.** 1998. Continuous human cell lines inducibly expressing hepatitis C virus structural and nonstructural proteins. Hepatology **28**:192–201. http://dx.doi.org/10.1002/hep.510280125.
23. **Shimakami T, Welsch C, Yamane D, McGivern D, Yi M, Zeuzem S, Lemon SM.** 2011. Protease inhibitor-resistant hepatitis C virus mutants with reduced fitness from impaired production of infectious virus. Gas-

troenterology 140:667–675. http://dx.doi.org/10.1053/j.gastro.2010.10.056.
24. Yi M, Villanueva RA, Thomas DL, Wakita T, Lemon SM. 2006. Production of infectious genotype 1a hepatitis C virus (Hutchinson strain) in cultured human hepatoma cells. Proc. Natl. Acad. Sci. U. S. A. 103:2310–2315. http://dx.doi.org/10.1073/pnas.0510727103.
25. Okamoto K, Mori Y, Komoda Y, Okamoto T, Okochi M, Takeda M, Suzuki T, Moriishi K, Matsuura Y. 2008. Intramembrane processing by signal peptide peptidase regulates the membrane localization of hepatitis C virus core protein and viral propagation. J. Virol. 82:8349–8361. http://dx.doi.org/10.1128/JVI.00306-08.
26. Weinlich S, Hüttelmaier S, Schierhorn A, Behrens SE, Ostareck-Lederer A, Ostareck DH. 2009. IGF2BP1 enhances HCV IRES-mediated translation initiation via the 3′UTR. RNA 15:1528–1542. http://dx.doi.org/10.1261/rna.1578409.
27. Bradrick SS, Nagyal S, Novatt H. 2013. A miRNA-responsive cell-free translation system facilitates isolation of hepatitis C virus miRNP complexes. RNA 19:1159–1169. http://dx.doi.org/10.1261/rna.038810.113.
28. Kao PN, Chen L, Brock G, Ng J, Kenny J, Smith AJ, Corthésy B. 1994. Cloning and expression of cyclosporin A- and FK506-sensitive nuclear factor of activated T cells: NF45 and NF90. J. Biol. Chem. 269:20691–20699.
29. Piñol-Roma S, Swanson MS, Gall JG, Dreyfuss G. 1989. A novel heterogeneous nuclear RNP protein with a unique distribution on nascent transcripts. J. Cell Biol. 109:2575–2587. http://dx.doi.org/10.1083/jcb.109.6.2575.
30. Sakamoto S, Aoki K, Higuchi T, Todaka H, Morisawa K, Tamaki N, Hatano E, Fukushima A, Taniguchi T, Agata Y. 2009. The NF90-NF45 complex functions as a negative regulator in the microRNA processing pathway. Mol. Cell. Biol. 29:3754–3769. http://dx.doi.org/10.1128/MCB.01836-08.
31. Barber GN. 2009. The NFAR's (nuclear factors associated with dsRNA): evolutionarily conserved members of the dsRNA binding protein family. RNA Biol. 6:35–39. http://dx.doi.org/10.4161/rna.6.1.7565.
32. Shi ST, Lee KJ, Aizaki H, Hwang SB, Lai MM. 2003. Hepatitis C virus RNA replication occurs on a detergent-resistant membrane that cofractionates with caveolin-2. J. Virol. 77:4160–4168. http://dx.doi.org/10.1128/JVI.77.7.4160-4168.2003.
33. Han SP, Tang YH, Smith R. 2010. Functional diversity of the hnRNPs: past, present, and perspectives. Biochem. J. 430:379–392. http://dx.doi.org/10.1042/BJ20100396.
34. Kaminski A, Hunt SL, Patton JG, Jackson RJ. 1995. Direct evidence that polypyrimidine tract binding protein (PTB) is essential for internal initiation of translation of encephalomyocarditis virus RNA. RNA 1:924–938.
35. Niepmann M. 1996. Porcine polypyrimidine tract-binding protein stimulates translation initiation at the internal ribosome entry site of foot-and-mouth-disease virus. FEBS Lett. 388:39–42. http://dx.doi.org/10.1016/0014-5793(96)00509-1.
36. Blyn LB, Towner JS, Semler BL, Ehrenfeld E. 1997. Requirement of poly(rC) binding protein 2 for translation of poliovirus RNA. J. Virol. 71:6243–6246.
37. Hwang B, Lim JH, Hahm B, Jang SK, Lee SW. 2009. hnRNP L is required for the translation mediated by HCV IRES. Biochem. Biophys. Res. Commun. 378:584–588. http://dx.doi.org/10.1016/j.bbrc.2008.11.091.
38. Tian B, Bevilacqua PC, Diegelman-Parente A, Mathews MB. 2004. The double-stranded-RNA-binding motif: interference and much more. Nat. Rev. Mol. Cell. Biol. 5:1013–1023. http://dx.doi.org/10.1038/nrm1528.
39. Liao HJ, Kobayashi R, Mathews MB. 1998. Activities of adenovirus virus-associated RNAs: purification and characterization of RNA binding proteins. Proc. Natl. Acad. Sci. U. S. A. 95:8514–8519. http://dx.doi.org/10.1073/pnas.95.15.8514.
40. Gomila RC, Martin GW, Gehrke L. 2011. NF90 binds the dengue virus RNA 3′ terminus and is a positive regulator of dengue virus replication. PLoS One 6:e16687. http://dx.doi.org/10.1371/journal.pone.0016687.
41. Isken O, Grassmann CW, Sarisky RT, Kann M, Zhang S, Grosse F, Kao PN, Behrens SE. 2003. Members of the NF90/NFAR protein group are involved in the life cycle of a positive-strand RNA virus. EMBO J. 22:5655–5665. http://dx.doi.org/10.1093/emboj/cdg562.
42. Isken O, Baroth M, Grassmann CW, Weinlich S, Ostareck DH, Ostareck-Lederer A, Behrens SE. 2007. Nuclear factors are involved in hepatitis C virus RNA replication. RNA 13:1675–1692. http://dx.doi.org/10.1261/rna.594207.

SCIENTIFIC REPORTS

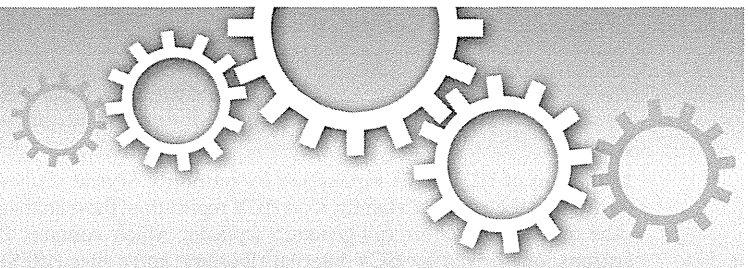

OPEN

SUBJECT AREAS:
HEPATITIS C VIRUS
DRUG REGULATION

Received
3 February 2014

Accepted
27 March 2014

Published
15 April 2014

Correspondence and requests for materials should be addressed to M.H. (mhonda@m-kanazawa.jp) or S.K. (skaneko@m-kanazawa.jp)

# The Acyclic Retinoid Peretinoin Inhibits Hepatitis C Virus Replication and Infectious Virus Release *in Vitro*

Tetsuro Shimakami[1], Masao Honda[1], Takayoshi Shirasaki[1], Riuta Takabatake[1], Fanwei Liu[1], Kazuhisa Murai[1], Takayuki Shiomoto[1], Masaya Funaki[1], Daisuke Yamane[2], Seishi Murakami[1], Stanley M. Lemon[2] & Shuichi Kaneko[1]

[1]Department of Gastroenterology, Kanazawa University Hospital, Kanazawa, Ishikawa 920-8641, Japan, [2]Lineberger Comprehensive Cancer Center and the Division of Infectious Diseases, Department of Medicine, The University of North Carolina at Chapel Hill, Chapel Hill, NC 27599-7292, USA.

**Clinical studies suggest that the oral acyclic retinoid Peretinoin may reduce the recurrence of hepatocellular carcinoma (HCC) following surgical ablation of primary tumours. Since hepatitis C virus (HCV) infection is a major cause of HCC, we assessed whether Peretinoin and other retinoids have any effect on HCV infection. For this purpose, we measured the effects of several retinoids on the replication of genotype 1a, 1b, and 2a HCV *in vitro*. Peretinoin inhibited RNA replication for all genotypes and showed the strongest antiviral effect among the retinoids tested. Furthermore, it reduced infectious virus release by 80–90% without affecting virus assembly. These effects could be due to reduced signalling from lipid droplets, triglyceride abundance, and the expression of mature sterol regulatory element-binding protein 1c and fatty acid synthase. These negative effects of Peretinoin on HCV infection may be beneficial in addition to its potential for HCC chemoprevention in HCV-infected patients.**

Hepatitis C virus (HCV) is a causative agent of chronic hepatitis, liver cirrhosis, and hepatocellular carcinoma (HCC); therefore, the eradication of HCV from an infected liver could reduce death from HCV-related liver disease. Combination therapy of PEGylated-interferon (PEG-IFN) and ribavirin has long been the standard of care for patients with chronic hepatitis C (CH-C); however, a sustained viral response (SVR) is obtained in only ~50% of treated patients infected with genotype 1 HCV[1]. Recently, several classes of direct-acting antiviral agents (DAAs) have entered into clinical use. In the United States, two NS3/4A protease inhibitors, telaprevir and boceprevir, were approved for use in combination with PEG-IFN and ribavirin in 2011. Although the addition of these DAAs dramatically improves the SVR rate, 20–30% of patients still fail to eradicate HCV due to breakthrough by drug-resistant mutants or null response to therapy[2]. More potent DAAs are currently in late clinical development and promise much higher SVR rates even in the absence of PEG-IFN therapy; however, HCV-related HCC is likely to continue to be a significant clinical issue for many years because it will take time for potent DAAs to be distributed worldwide.

Peretinoin (generic name code: NIK-333) is an oral acyclic retinoid with a vitamin A-like structure that targets retinoid nuclear receptors, such as retinoid X receptor and retinoic acid receptor. The oral administration of Peretinoin significantly reduces the incidence of post-therapeutic HCC recurrence and improves the survival rate of patients in clinical trials[3,4]. In addition, Peretinoin prevents the development of hepatoma in several different hepatoma models[5,6]. Larger-scale clinical studies are currently ongoing in various countries to confirm its clinical efficiency. Depending on the results of these studies, Peretinoin may be used in CH-C patients to prevent HCC. Therefore, we sought to understand the effect of Peretinoin on HCV replication.

Peretinoin is categorised as a vitamin A or retinoid compound, and conflicting reports have described the effects of vitamin A compounds on HCV replication. One report showed that 3 retinoids, 9-cis retinoic acid (RA), 13-cis RA, and all-trans RA (ATRA), suppressed the replication of a sub-genomic HCV replicon[7]. However, vitamin A also reportedly enhances the replication of genome-length HCV in Huh-7 cells[8]. Here, we describe the impact of Peretinoin on different steps of the HCV life cycle, including translation, RNA amplification, virus assembly, and secretion, and its impact on host lipid metabolism *in vitro*. Our results clearly demonstrate that Peretinoin inhibits HCV RNA amplification and virus release by altering lipid metabolism.

## Results

**Inhibition of HCV RNA replication by retinoids.** Several studies have tested the effects of vitamin A on HCV replication; these studies used a sub-genomic or full-genomic replicon, which contains 2 cistrons, one driven by HCV internal ribosome entry sites (IRES) and the other by encephalomyocarditis virus IRES[7,8]. We reported the usefulness of HCV genomes containing *Gaussia princeps* luciferase (GLuc) between p7 and NS2, followed by foot-and-mouth disease virus 2A, to monitor HCV RNA replication[9,10], and this system is closer to physiological HCV replication than the bicistronic replicon systems (Fig. 1A). In addition to GLuc-containing HCV genomes in the backbone of genotype 1a H77S.3, a chimeric clone of H77S and genotype 2a JFH1, HJ3-5[11], with structural proteins from H77S and non-structural proteins from JFH1, we also constructed GLuc-containing genomes in the backbone of genotype 1b N[12] and 2a JFH1[13] and confirmed their efficient replication in Huh-7.5 cells. Importantly, all of the strains used here are derived from cDNA clones that are infectious to chimpanzees.

We initially examined the effects of 4 different retinoids, namely ATRA, 9-cis RA, 13-cis RA, and Peretinoin, on HCV replication by using these 4 HCV genomes containing GLuc, according to the use of GLuc activity as an indicator of RNA replication, and the structures of each retinoid were shown in Supplementary Fig. S1 online. Peretinoin inhibited the replication of H77S.3/GLuc2A in a dose-dependent manner (Fig. 1B). As the other retinoids also suppressed HCV replication, we determined the antiviral half maximal effective concentrations ($EC_{50}$s) of these retinoids for each HCV genotype. Whilst Peretinoin showed the strongest antiviral effect on all genotypes tested, ATRA exerted a moderate effect, and 9-cis and 13-cis RA generated a weaker effect (Table 1). Especially, Peretinoin suppressed the RNA replication of H77S.3/GLuc2A most efficiently and its $EC_{50}$ was 9 μM.

We also determined the half maximal cytotoxicity concentrations ($CC_{50}$s) of these retinoids in H77S.3/GLuc2A-replicating Huh-7.5 cells by using the WST-8 assay, which reflects cell number. The $CC_{50}$s of ATRA, 9-cis RA, and 13-cis RA were more than 100 μM; however, the $CC_{50}$ of Peretinoin was 68 μM when the cells were treated for 72 h (Table 2). Although Peretinoin had a slightly negative impact on cell growth, as it showed the strongest antiviral effect and may be used for HCC chemoprevention in HCV-infected patients in the future, we focused upon the action of Peretinoin among these retinoids.

**Inhibition of HCV RNA replication by Peretinoin.** We examined the time dependence of the antiviral effect of Peretinoin. After HCV RNA transfection, we treated the transfected cells with Peretinoin at a range of concentrations (10–40 μM) and monitored RNA replication every 24 h until 72 h. Peretinoin started to show an antiviral effect from 24 h after treatment, which continued until 72 h. Peretinoin suppressed RNA replication in a time-dependent manner for all genotypes tested (Fig. 1C).

We also examined whether Peretinoin could also suppress RNA replication in a sub-genomic replicon system (Fig. 1D), in which infection should not occur due to the lack of structural proteins. Peretinoin was also able to suppress RNA replication in a dose-dependent manner in bicistronic sub-genomic RNA-transfected cells (Fig. 1E).

Importantly, when we treated HCV (H77S.3/GLuc2A)-replicating and HCV-non-replicating Huh-7.5 cells with Peretinoin at a range of concentrations (5–50 μM), the cell numbers were identical under the conditions tested (Fig. 1F).

As Peretinoin could suppress GLuc activity itself, we then examined directly its antiviral effect in the context of an HCV genome lacking the GLuc genome. For this purpose, Huh-7.5 cells infected with cell culture-derived HCV (HCVcc) of HJ3-5 were treated with different concentrations of Peretinoin. When we monitored HCV RNA replication by using quantitative real-time detection-polymerase chain reaction (RTD-PCR) (Fig. 2A) and protein expression by western blotting for the HCV core protein (Fig. 2B, see Supplementary Fig. S2 online), Peretinoin suppressed RNA replication and protein expression in a dose-dependent manner, which is consistent with the GLuc activity results. We also tested infectious virus production from Peretinoin-treated cells using a conventional focus forming unit (FFU) assay, and found that Peretinoin also reduced this in a dose-dependent manner (Fig. 2C).

**Effect of Peretinoin on translation driven by HCV IRES.** We also tested the effect of Peretinoin on translation directed by HCV IRES. For this purpose, we used a mini-genome RNA which has, sequentially, the HCV 5′-untranslated region (UTR), GLuc, and HCV 3′-UTR, and cap-*Cypridina* luciferase (CLuc)-polyA RNA as a control (see Supplementary Fig. S1 online). After we treated Huh-7.5 cells with different concentrations of Peretinoin for 24 h, we co-transfected the cells with these RNAs and measured GLuc and CLuc activity every 3 h from 3 to 12 h. When we normalised GLuc activity to CLuc activity at each time point, we did not observe a significant difference among the cells treated with the different concentrations of Peretinoin (see Supplementary Fig. S3 online), suggesting that Peretinoin does not have an effect on protein expression directed by HCV IRES.

**Effect of Peretinoin on cellular interferon signalling.** We hypothesised that the suppression of RNA replication by Peretinoin could be due to the activation or enhancement of cellular interferon (IFN) signalling. To examine this, we treated HCV (H77S.3/GLuc2A)-non-replicating and HCV-replicating Huh-7.5 cells with either IFNα-2b (10 IU/mL) or Peretinoin (10–40 μM) and monitored the expression of total and phosphorylated signal transducer and activator of transcription 1 (STAT1). Peretinoin did not alter the expression of either total or phosphorylated STAT1 in HCV-non-replicating Huh-7.5 cells or HCV-replicating cells (see Supplementary Fig. S4 online). In addition, Peretinoin did not further enhance the amount of phosphorylated STAT1 activated by IFNα-2b in HCV-non-replicating Huh-7.5 cells or HCV-replicating cells (see Supplementary Fig. S4 online). These data suggest that Peretinoin suppresses RNA replication without either activating or enhancing cellular IFN signalling.

**Impact of Peretinoin on lipid metabolism.** As lipid metabolism has an important role in various aspects of HCV infection[14–16], we examined the impact of Peretinoin on lipid metabolism. However, as it is sometimes difficult to detect small changes in lipid metabolism, we tested the effect of Peretinoin under oleic acid (OA) treatment, which amplifies changes in lipid metabolism. We treated H77S.3/GLuc2A-replicating Huh-7.5 cells with 40 μM Peretinoin and 250 μM OA, fixed and stained the cells with BODIPY 493/503 for lipid droplets (LDs) and 4′, 6-diamidino-2-phenylindole (DAPI) for nuclei, and used an anti-core protein antibody to detect HCV. When we stained LDs in the presence of 250 μM OA and the absence of Peretinoin, we observed intense signals (Fig. 3A); however, when it was accompanied with 40 μM Peretinoin, the signals from LDs were dramatically reduced, and at the same time, the expression of HCV core protein was also down-regulated (Fig. 3B). When we quantitated the signal strength from LDs and HCV core protein in 4 different fields, Peretinoin significantly reduced the signals from LDs and HCV core protein (two-tailed Student's t test, $p<0.0001$ for each) (Fig. 3C). This reduction was also confirmed by the quantitation of the 5 cells which were positive for both LDs and HCV core (see Supplementary Fig. S5 online). The reduced expression of HCV core protein was also observed by western blot analysis (Fig. 3D, see Supplementary Fig. S6 online). We next investigated the

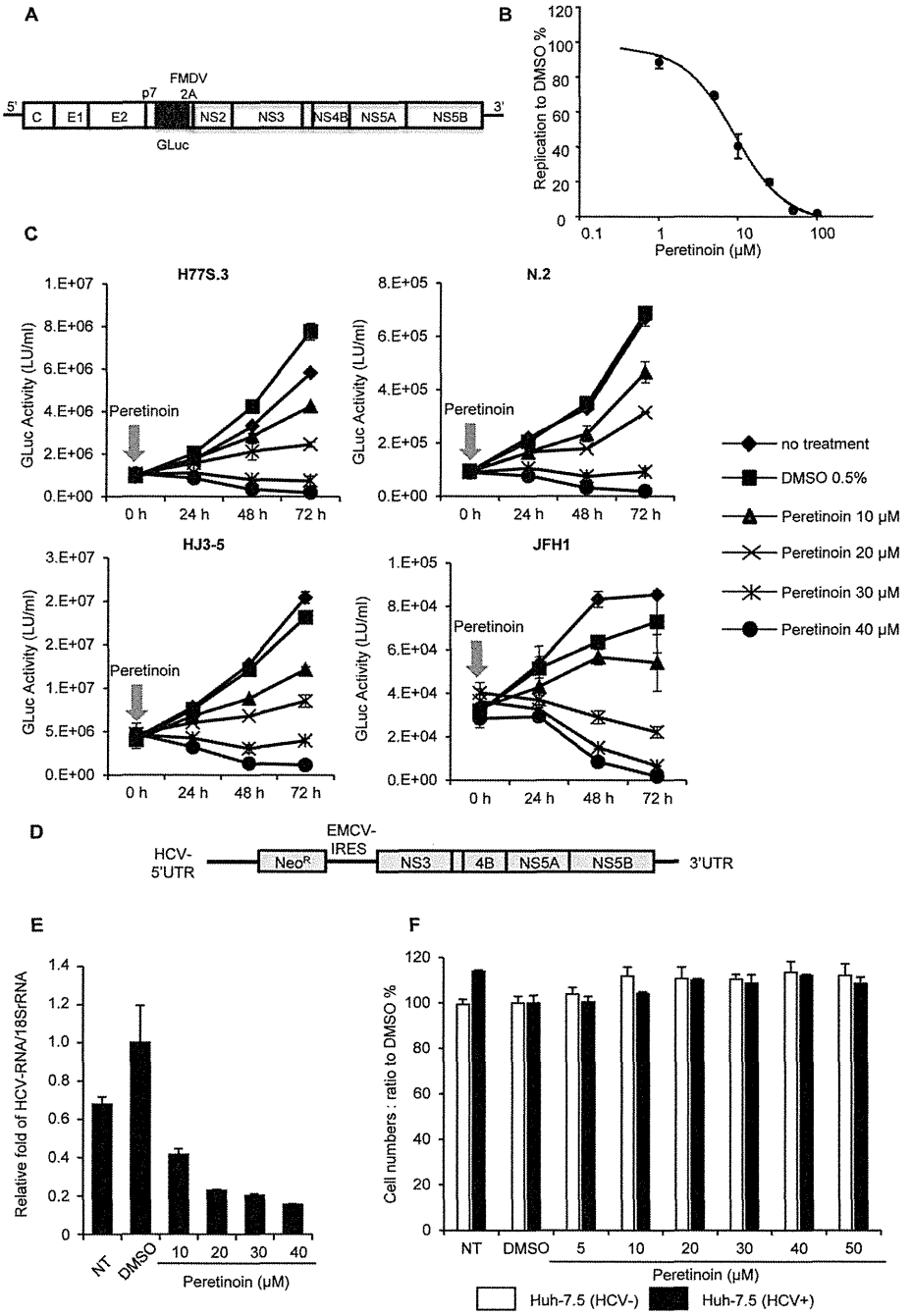


**Figure 1 | Antiviral effects of several retinoids and their effects on cell growth.** (A) Schematic representation of the GLuc-containing HCV genome. (B) Huh-7.5 cells were transfected with H77S.3/GLuc2A RNA, and 48 h later, 0.5% DMSO or Peretinoin was added at concentrations ranging from 1 to 100 μM. Fresh medium containing Peretinoin was added every 24 h, and 72 h after adding Peretinoin, secreted GLuc activity was measured. The GLuc activity from Peretinoin-treated cells was normalised to that with DMSO treatment. Data show the mean inhibition to DMSO treatment in each concentration of Peretinoin ± SD from 3 independent experiments. (C) Huh-7.5 cells were transfected with H77S.3/GLuc2A, N.2/GLuc2A, HJ3-5/GLuc2A, and JFH1/GLuc2A RNAs, and 48 h later, 0.5% DMSO or Peretinoin was added at the indicated concentrations. The medium was collected and replaced with fresh medium every 24 h until 72 h. GLuc activity was determined at each time point. The results shown represent the mean GLuc activity ± SD from 3 different plates. (D) Schematic representation of the bicistronic sub-genomic HCV RNA (E) Huh-7.5 cells were transfected with bicistronic sub-genomic RNA. At 48 h later, the transfected cells were treated with the indicated concentrations of Peretinoin for 72 h. Quantification of HCV RNA and 18S rRNA levels was performed and relative HCV RNA abundance normalised to the amount of 18S rRNA is presented as fold change ± SD compared to DMSO-treated cells from 3 independent experiments. (F) Huh-7.5 cells were transfected with H77S.3/GLuc2A RNA, and 7 days later, HCV (H77S.3/GLuc2A)-replicating Huh-7.5 cells, depicted as 'HCV+', were treated with the indicated concentrations of Peretinoin and HCV-non-replicating Huh-7.5 cells, depicted as 'HCV-', were also treated in a same way. At 72 h after Peretinoin treatment, cell numbers were determined by using a Cell Counting Kit-8. Data represent relative cell numbers ± SD from 3 independent experiments to DMSO-treated cells. EMCV, Encephalomyocarditis virus; Neo$^R$, Neomycin resistance gene; NT, no treatment.